# Dual-Layered MIMO Transmission for Increased Bandwidth Efficiency

Christos Masouros, *Senior Member, IEEE*, and Lajos Hanzo, *Fellow, IEEE*

*Abstract*—A dual-layered downlink transmission scheme is proposed for intrinsically amalgamating multiple-input–multiple-output (MIMO) spatial multiplexing (SMX) with spatial modulation (SM). The proposed scheme employs a classic SMX transmission that is known to offer superior bandwidth efficiency (BE) compared with SM. We exploit receive-antenna-based SM (RSM) on top of this transmission as an enhancement of the BE. The RSM here is applied to the combined spatial and power-level domain not by activating and deactivating the RAs but rather by choosing between two power levels $\{P_1, P_2\}$ for the received symbols in these antennas. In other words, the combination of symbols received at a power level $P_1$ carries information in the spatial domain in the same manner as the combination of nonzero elements in the receive symbol vector carries information in the RSM transmission. This allows for the coexistence of RSM with SMX, and the results show increased BE for the proposed scheme compared with both SMX and SM. To characterize the proposed scheme, we carry out a mathematical analysis of its performance, and we use this to optimize the ratio between $P_1$ and $P_2$ for attaining the minimum error rates. Our analytical and simulation results demonstrate significant BE gains for the proposed scheme compared with conventional SMX and SM.

*Index Terms*—Multiple-input–multiple-output systems, spatial modulation (SM), spatial multiplexing (SMX), transmit precoding (TPC).

## I. INTRODUCTION

**M**ULTIANTENNA-aided transceivers have been shown to improve the capacity of the wireless channel by means of spatial multiplexing (SMX) [1]. For the multiuser downlink (DL), transmit precoding (TPC) schemes have been shown to improve both the attainable power efficiency (PE) and the cost of mobile terminals by shifting the signal processing complexity to the base stations (BSs). Numerous TPC solutions exist, ranging from highly complex capacity achieving nonlinear dirty paper coding techniques [2] and their low-complexity suboptimal counterparts in the form of Tomlinson–Harashima precoding [3]–[6] to linear TPC schemes based on channel inversion [7]–[12] that offers the lowest complexity, albeit at an inferior performance. The performance–complexity tradeoffs between the above TPC have been thoroughly studied in the literature. More recently, it has been shown that the family of linear techniques exhibits a close-to-optimal performance in the large-scale multiple-input–multiple-output (MIMO) region [13]–[15]. Accordingly, we focus on the class of low-complexity closed-form linear TPC [7]–[12] due to their favorable performance–complexity tradeoff and practical relevance.

More recently, spatial modulation (SM) has been conceived for implicitly encoding information in the index of the specific antenna activated for the transmission of the modulated symbols, offering a low-complexity design alternative [16]. Its central benefits include the absence of interantenna interference (IAI) and the fact that it only requires a subset (down to one) of radio-frequency (RF) chains compared with SMX. Accordingly, the interantenna synchronization is also relaxed. Early work has focused on the design of receiver algorithms for minimizing the bit error ratio (BER) of SM at low complexity [16]–[21]. The work spans from matched filtering as a low-complexity technique for detecting the antenna index used for SM [16] to the maximum likelihood (ML) [20] with a significantly reduced complexity compared with classic SMX ML detectors, including compressive sensing approaches [18] and performance analyses [19]. Reduced-space sphere detection has also been proposed for SM in [21] for further complexity reduction where a generalized SM transmission was also explored [22]. In addition to receive processing, recent work has also proposed constellation shaping for SM [23]–[33]. Specifically, the work on this topic has focused on three main directions: shaping and optimization of the spatial constellation, i.e., the legitimate sets of activated transmit antennas (TAs) [23], modulation constellation shaping [24]–[28] for the SM and space shift keying transmission, where the constellation of the modulated bits is optimized, and joint spatial and modulation constellation shaping, in the form of optimizing the received constellation [29]–[33].

Closely related work has focused on applying the concept of SM to the receive antennas (RAs) of the communication link, as opposed to the TAs as per the above approaches, forming the RA-based spatial modulation (RSM) concept [36]–[39]. By means of TPC, this technique targets a specific subset of RAs, which receive information symbols, whereas the rest of the RAs

C. Masouros is with the Department of Electrical and Electronic Engineering, University College London, London WC1E 7JE, U.K. (e-mail: chris.masouros@ieee.org).

L. Hanzo is with the School of Electronics and Computer Science, University of Southampton, Southampton SO17 1BJ, U.K. (e-mail: lh@ecs.soton.ac.uk).

receive only noise. This may be achieved by using zero-forcing (ZF) TPC and transmitting a combination of information symbols and zeros to the RAs, depending on the spatial symbols to convey. As opposed to conventional SM where a subset of RF chains is deployed, here, all TAs and RAs are active and therefore there are no RF chain reductions. Still, the computational complexity of the receivers is drastically reduced, where simply the indexes of the targeted RAs have to be detected, and the classic symbols received at the activated RAs are then demodulated.

Inspired by the above RSM philosophy, here, we propose a dual-layered transmission (DLT) scheme, which intrinsically amalgamates a full spatial multiplexing (SMX) with SM. First, we note that since, for RSM, all TAs and RAs are active, there are no RF chain reductions, and this motivates the full SMX approach. To accommodate the SMX, we apply an SM to the combined spatial and receive-power domain, where instead of sending a combination of information symbols and zero power to the RAs, we apply two different power levels for distinguishing between the "active" and "inactive" RAs. In this manner, the spatial symbols are formed based on the power levels detected. We demonstrate that this improves the bandwidth efficiency (BE) with respect to SMX and SM. Against this state of the art, we list the main contributions of this paper.

- We propose a new DLT scheme based on linear TPC that improves the BE by jointly exploiting the benefits of SMX and RSM.
- We provide the performance analysis of the proposed technique based on the pairwise error probability (PEP) between different constellation points in the supersymbol constellation formed by the combination of the spatial constellation of RSM and the classic modulation constellation of SMX.
- We use the above results for analytically deriving the optimum power ratio between the two sets of antennas that carry the spatial symbol for the proposed scheme for minimizing the probability of detection errors.
- We calculate and compare analytically the complexity of the conventional and proposed techniques, and quantify the performance–complexity tradeoff of conventional and proposed schemes, by introducing a PE metric that combines the BE, transmit power, and complexity, to prove the enhanced tradeoff for the proposed scheme.

*Remark 1:* It should be noted that, while this paper focuses on a single-link scenario, the proposed technique can be readily extended to a multiuser DL scenario, where the DLT and the related RSM take place on a per-user basis, as facilitated by the ZF-TPC employed at the BS.

*Remark 2:* The proposed scheme does not consist of a power allocation scheme in the sense of allocating power according to the quality-of-service (QoS) requirements of the user. This power allocation may be applied in addition to the proposed scheme in the multiuser scenario, where different users with different QoS requirements employ different sets of power levels $\{P_1, P_2\}$ accordingly.

*Remark 3:* To facilitate the proposed power-level modulation, this paper focuses on phase shift keying (PSK) in terms

of the classical symbol modulation. Its adaptation to quadrature amplitude modulation (QAM) is not trivial since the variability of the power levels for the classically modulated symbols would hinder the detection of the power levels of the spatially modulated symbols. Nevertheless, even for PSK modulation, our results illustrate a wide range of achievable BEs for the proposed scheme and an improved performance compared with classical SMX associated with both PSK and QAM for the same BE.

The remainder of this paper is organized as follows. Section II presents the MIMO system model and introduces the RSM transmission philosophy. Section III details the proposed DLT scheme, whereas in Section IV, we present our analytical study of the performance attained and the analytical optimization of the power ratio for the proposed scheme. Section V detail the complexity calculation and the study of the attainable PE. Finally, Section VI presents our numerical results, whereas our conclusions are offered in Section VII.

## II. System Model and Receive-Antenna-Based Spatial Modulation

### A. System Model

Consider a MIMO system, where the transmitter and receiver are equipped with $N_t$ and $N_r$ antennas, respectively. For simplicity, unless stated otherwise, in this paper, we assume that the transmit power budget is limited as $P = 1$. For the case of the closed-form TPCs of [7]–[12], it is required that $N_t \geq N_r$. The given channel is modeled as follows:

$$\mathbf{y} = \mathbf{H}\mathbf{t} + \mathbf{w} \qquad (1)$$

where $\mathbf{y}$ is the vector of received symbols in all RAs, and $\mathbf{H}$ is the MIMO channel vector with elements $h_{m,n}$ representing the complex channel coefficient between the $n$th TA and the $m$th RA. Furthermore, $\mathbf{t}$ is the vector of precoded transmit symbols that will be discussed in the following, and $\mathbf{w} \sim \mathcal{CN}(0, \sigma^2 \mathbf{I})$ is the additive white Gaussian noise (AWGN) component at the receiver, with $\mathcal{CN}(\mu, \sigma^2)$ denoting the circularly symmetric complex Gaussian distribution with a mean of $\mu$ and a variance of $\sigma^2$.

### B. Receive-Antenna-Based Spatial Modulation

The block diagram of RSM as proposed in [36] is shown in Fig. 1(a). RSM targets a subset of the RAs by sending information symbols to these RAs and zero power to the rest of the RAs. While for RSM all RAs have to be on to detect the arrival of information symbols, for coherence with the SM literature, we shall refer to the antennas as "active" and "inactive," depending on whether they do or do not receive information symbols, respectively. The specific combination of RAs that do receive symbols implicitly conveys the symbol transmitted in the spatial domain. The above RA subset transmission is achieved by forming a supersymbol vector in the form $\mathbf{s}_m^k = \mathbf{e}_k b_m = [0, \ldots, b_{m_1}, \ldots, 0, \ldots, b_{m_2}, \ldots, 0]^T$ with $N_a$ nonzero elements, where $\mathbf{e}_k$ is a diagonal matrix of size
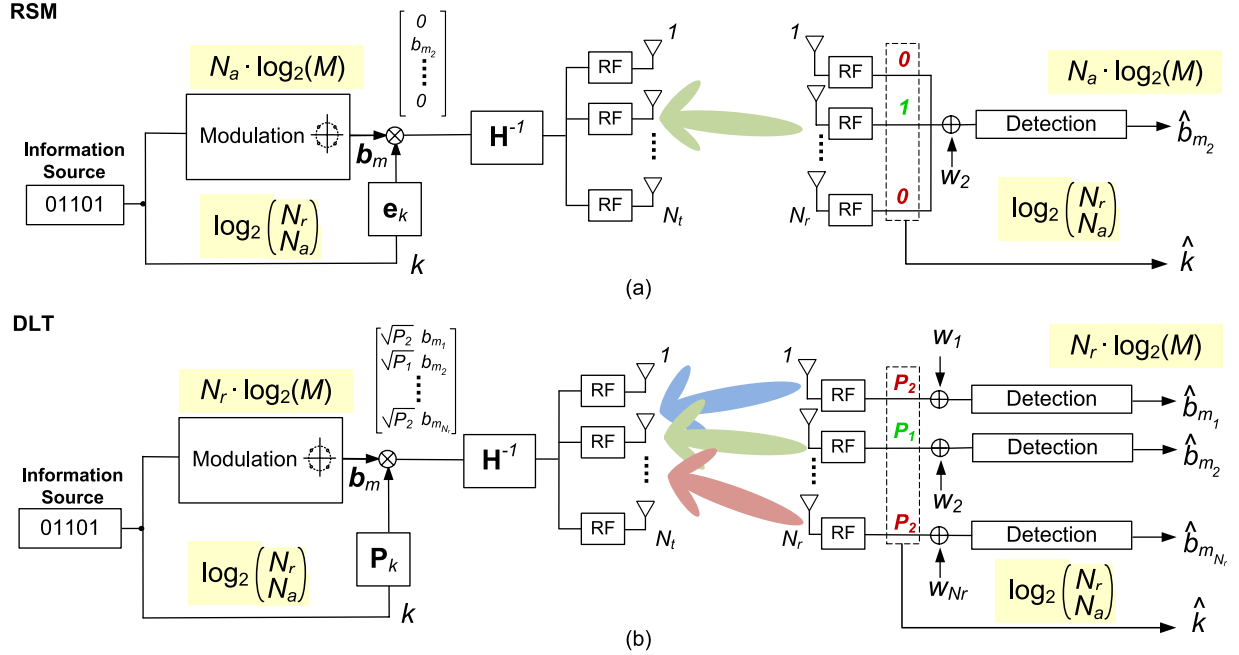
Fig. 1. Block diagram of (a) RSM and (b) DLT transmission.

$N_r$ with elements taken from the set $\{1, 0\}$ on its diagonal, which represents the RAs that are activated. The notation $[\cdot]^T$ denotes the transpose operator. Here, $b_{m_i}, m_i \in \{1, \ldots, M\}$ is a symbol taken from an $M$-order modulation alphabet that represents the transmitted waveform in the baseband domain conveying $\log_2(M)$ bits and $k$ represents the index of the $N_a$ activated RAs (the index of the nonzero elements in $\mathbf{s}_m^k$) conveying $\log_2\binom{N_r}{N_a}$ bits in the spatial domain. Accordingly, the total number of bits conveyed per supersymbol for RSM is

$$\beta = N_a \log_2(M) + \log_2 \binom{N_r}{N_a}. \tag{2}$$

The transmitter then sends

$$\mathbf{t} = f\mathbf{T}\mathbf{s}_m^k \tag{3}$$

where $\mathbf{T} = \mathbf{H}^H(\mathbf{H}\mathbf{H}^H)^{-1}$ is the ZF-TPC [7] that preserves the form of $\mathbf{s}_m^k$ at the receiver. The factor $f = \sqrt{1/\text{tr}(\mathbf{T}\mathbf{T}^H)}$, where $\text{tr}(\cdot)$ denotes the trace operator and normalizes the average transmit power to $P = 1$. The received symbol vector can be written as

$$\mathbf{y} = f\mathbf{H}\mathbf{T}\mathbf{s}_m^k + \mathbf{w} = f\mathbf{s}_m^k + \mathbf{w} \tag{4}$$

where, clearly, all IAI is removed. At the receiver, a joint ML detection of both the RA index and the transmit symbol is obtained by the following minimization:

$$[\hat{s}_m, \hat{k}] = \arg\min_i \|\mathbf{y} - \dot{\mathbf{y}}_i\|$$
$$= \arg\min_{m_i, k_i} \|\mathbf{y} - f\mathbf{H}\mathbf{T}\mathbf{s}_{m_i}^{k_i}\| \tag{5}$$

where $\|\mathbf{x}\|$ denotes the norm of vector $\mathbf{x}$, and $\dot{\mathbf{y}}_i$ is the $i$th constellation point in the received SM constellation. A low-

complexity decoupled approach is also proposed in [36], where the first active antenna indexes are detected in the form of

$$\hat{k} = \arg\max_{j \in \mathcal{J}} \sum_{i=1}^{N_a} |y_{j,i}|^2 \tag{6}$$

where $\mathcal{J}$ denotes the set of symbols in the spatial domain, and then, the classic modulated symbols are detected by

$$\hat{b}_{m_i} = \arg\min_{n_i \in \mathcal{Q}} |y_{\hat{k},i}/f - b_{n_i}|^2 \tag{7}$$

where $\mathcal{Q}$ denotes the modulation constellation, and $b_{n_i}$ are the symbols in the modulated symbol alphabet. For reasons of computational complexity, we shall focus on the latter detector in this paper.

## III. PROPOSED DUAL-LAYERED TRANSMISSION

From the above system description, it can be seen that for the particular case of RSM, while the detection complexity is clearly reduced with respect to SMX, there are no savings in RF complexity since all $N_r$ RAs have to be activated and receiving for the detection in (6) and (7). Still, by forming a subset of beams towards the receiver, as shown in Fig. 1(a), the BE, i.e., the number of bits per channel use, is generally lower for RSM than for SMX. Motivated by this, we propose a dual-layered approach combining SMX with RSM, where the BE of conventional SMX MIMO transmission is strictly enhanced by encoding spatial bits in the RSM fashion in the received power domain, by selecting two distinct, nonzero power levels for the transmitted supersymbols instead of the "on–off" RSM transmission in the $\{1, 0\}$ manner. This allows for nonzero elements throughout the supersymbol vector $\mathbf{s}_m^k$,

hence supporting a full SMX transmission in the modulated signal domain. The block diagram of the proposed DLT is shown in Fig. 1(b).

*1) Transmitter:* Here, we employ a full data vector in the form of $\mathbf{b}_m = [b_{m_1}, b_{m_2}, \ldots, b_{m_{N_r}}]^T$, with all elements being nonzero, and the encoding of the spatial bits is achieved by allocating different power levels to the received symbols according to the spatial symbol $k$, by applying the power allocation matrix $\mathbf{P}_k$, i.e.,

$$\mathbf{s}_m^k = \mathbf{P}_k \mathbf{b}_m = [s_{m_1}, s_{m_2}, \ldots, s_{m_{N_r}}]^T \quad (8)$$

with

$$\mathbf{P}_k = \begin{bmatrix} \sqrt{p_1} & 0 & \cdots & 0 \\ 0 & \sqrt{p_2} & \cdots & 0 \\ \vdots & \vdots & \ddots & \vdots \\ 0 & 0 & \cdots & \sqrt{p_{N_r}} \end{bmatrix} \quad (9)$$

where $p_i, i \in [1, N_r]$ are taken from the set $\{P_1, P_2\}$ according to the spatial symbol $k$. Note that classic QoS-based power allocation can be applied in addition to this process by employing an additional power allocation matrix on top of (9). The receiver can then remove this additional matrix by simple inversion, in order to detect the spatial symbol. For notational simplicity and to keep the focus of the discussion on the proposed concept, we neglect QoS-based power allocation.

*2) Receiver:* At the receiver side, the explicit knowledge of the power levels $\{P_1, P_2\}$ is not required, as long as the detector can distinguish between the two power levels. The received signal of (4) can be decomposed as

$$y_p = f\sqrt{P_1} b_{m_p} + w_p, p \in \mathcal{A} \quad (10)$$

$$y_q = f\sqrt{P_2} b_{m_q} + w_q, q \in \mathcal{I} \quad (11)$$

where $\mathcal{A}$ and $\mathcal{I}$ denote the sets of "active" and "inactive" antennas, respectively. Hence, the receive processing is similar to the conceived one for RSM, with the difference that the classic modulated symbols of all RAs have to be detected, as opposed to those of $N_a$ antennas only for RSM. Accordingly, the receiver first detects the set of antennas with the highest received power levels and then detects the classic modulated symbols at all RAs according to

$$\hat{k} = \arg\max_{j \in \mathcal{J}} \sum_{i=1}^{N_a} |y_{j,i}|^2 \quad (12)$$

where $\mathcal{J}$ denotes the set of symbols in the spatial domain, and

$$\hat{\mathbf{b}}_m = \arg\min_{n \in \mathcal{Q}} |\mathbf{y}/f - \mathbf{b}_n|^2 \quad (13)$$

where $\mathcal{Q}$ denotes the classic modulation constellation, and $b_n$ are the symbols in the modulated symbol alphabet.

TABLE I
BE IN BITS PER CHANNEL USE FOR SMX, RSM, AND DLT

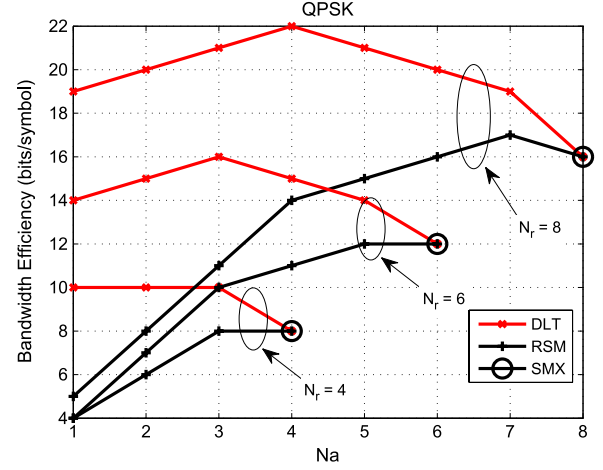| | Bandwidth Efficiency (BE) |
|---|---|
| SMX | $\beta = N_r \log_2(M)$ |
| RSM | $\beta = N_a \log_2(M) + \log_2\binom{N_r}{N_a}$ |
| DLT | $\beta = N_r \log_2(M) + \log_2\binom{N_r}{N_a}$ |



Fig. 2. BE versus $N_a$ for SMX, RSM, and DLT using the expressions of Table I.

### A. Bandwidth Efficiency

Clearly, the encoding process in (8) and (9) encodes $N_r \log_2(M)$ bits in the modulated symbol domain and an additional $\log_2\binom{N_r}{N_a}$ bits in the spatial domain. This results in a total of

$$\beta = N_r \log_2(M) + \log_2\binom{N_r}{N_a} \quad (14)$$

bits per transmitted supersymbol for DLT, which is strictly greater than that for SMX and RSM. Here, the notation $N_a$ denotes the number of antennas receiving symbols at the power level $P_1$. We should emphasize that, although all RAs are active for both RSM and the proposed DLT, for coherence with the SM literature, we shall adhere to the terms "active" and "inactive" to indicate the antennas receiving $\{1, 0\}$ and $\{P_1, P_2\}$ for RSM and DLT, respectively. A comparison of the BEs of SMX, RSM, and DLT is shown in Table I, where it can be seen that the proposed DLT approach has an improved BE compared with the conventional approaches. This is quantified in Fig. 2, where the BE is expressed in terms of bits per channel use is shown with increasing numbers of "active" antennas $N_a$ for MIMO links with $N_r = 4$, $N_r = 6$, and $N_r = 8$, where the clear benefits of the proposed approach can be seen. It can be observed that the additional BE of DLT compared with SMX can be maximized by appropriately selecting the number of activated antennas according to

$$\tilde{N}_a = \arg\max_{N_a} \log_2\binom{N_r}{N_a} = N_r/2 \quad (15)$$

which is demonstrated in the figure.

## B. Symbol Power Levels

With regard to the resulting BER performance, the set of spatial power levels $\{P_1, P_2\}$ must be carefully selected so that they satisfy a combination of two constraints.

1) There is sufficient separation between the two power levels $P_1, P_2$ for correct detection of the "active" antennas and hence the spatial symbol $k$ in the presence of noise.
2) The symbols received with $P_2 < P_1$ that dominate the BER of the modulated symbol detection must experience a sufficiently high signal-to-noise ratio (SNR) that is adequate for reliable demodulation.

Let us therefore define the power ratio

$$\alpha = \frac{P_2}{P_1} \tag{16}$$

as the ratio between the two power levels transmitted, which is optimized in the following results. Since $N_a$ symbols are transmitted with power $P_1$ and the remaining $N_r - N_a$ symbols have power of $P_2$, given a total power budget of $P = 1$, we have

$$P_1 = \frac{1}{(N_r - N_a)\alpha + N_a} \tag{17}$$

$$P_2 = \frac{\alpha}{(N_r - N_a)\alpha + N_a}. \tag{18}$$

Clearly, since the power levels $P_1, P_2$ influence the reliability of detection for the modulated symbols and since the ratio $\alpha$ determines the detection reliability of the spatial symbols, $\alpha$ can be optimized for best BER performance. In the following, we derive a closed-form expression for the optimum $\alpha$ value for an $M$-order PSK modulation, where it can be seen that this optimum value is independent of both $N_r$ and of $N_a$.

*Remark:* Regarding the effect of the above on the transmit power distribution, we note that the power imbalance discussed refers to the information symbols $\mathbf{s}_m^k$ and does not translate to a power imbalance for the transmit symbols $\mathbf{t}$. Indeed, the ZF-precoded transmit symbols have the same average transmit power, constrained by the scaling factor $f$ as shown above, which is valid for both the proposed DLT and for the conventional SMX, and these transmit symbols exhibit the same power distribution for both techniques. In other words, the proposed scheme does not impact the design of the power amplifiers used at the transmitter.

To verify the above, Fig. 3 shows the probability density function (pdf) of the normalized transmit power per antenna for both SMX and DLT in a $(8 \times 4)$ element MIMO system. It can be seen that, as expected, both techniques show the same distribution of transmit power.

## IV. DUAL-LAYERED TRANSMISSION PERFORMANCE ANALYSIS AND OPTIMUM POWER RATIO $\alpha$

### A. Probability of Error

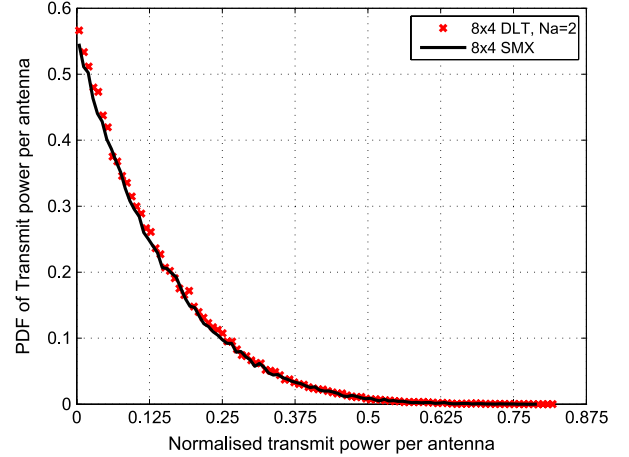Here, we carry out a performance analysis for the proposed DLT scheme by deriving the PEP between the pair of symbols



Fig. 3. PDF of transmit power per antenna for a $(8 \times 4)$ MIMO with SMX and DLT and QPSK with Rayleigh fading.

$\mathbf{s}_m^k$ and $\mathbf{s}_n^l$ in the superimposed spatial and classic modulation constellations, following the analysis in [36]. Accordingly, we define the PEP as $\mathcal{P}(\mathbf{s}_m^k \to \mathbf{s}_n^l)$ and use the union bound for the average bit error probability $P_e$, which is expressed as

$$P_e \leq \frac{1}{\beta} E \left\{ \sum_{\mathbf{s}_m^k \in \mathcal{B}} \sum_{\mathbf{s}_n^l \in \mathcal{B} \neq \mathbf{s}_m^k} d\left(\mathbf{s}_m^k, \mathbf{s}_n^l\right) \mathcal{P}\left(\mathbf{s}_m^k \to \mathbf{s}_n^l\right) \right\} \tag{19}$$

where $d(\mathbf{s}_m^k, \mathbf{s}_n^l)$ is the Hamming distance between the bit representations of symbols $\mathbf{s}_m^k, \mathbf{s}_n^l$ and $\mathcal{B} = \mathcal{J} \cup \mathcal{Q}$ is the super-symbol constellation defined as the union of the spatial domain constellation and the classic modulation constellation. We have used the operator $\cup$ to define the union of sets. For the PEP, we have the following theorem.

*Theorem 1:* The PEP $\mathcal{P}(\mathbf{s}_m^k \to \mathbf{s}_n^l)$ for DLT can be expressed as

$$\mathcal{P}\left(\mathbf{s}_m^k \to \mathbf{s}_n^l\right) = Q\left( \frac{f}{\sqrt{N_0}} \left( 1 - \sum_{i=1}^{N_r} \sqrt{p_{k_i} p_{l_i}} \mathcal{R}\{b_{m_i}^* b_{n_i}\} \right) \right) \tag{20}$$

where $Q(\cdot)$ denotes the Gaussian $q$-function [42], $\mathcal{R}\{\cdot\}$ denotes the real part of a number, $(\cdot)^*$ denotes the complex conjugate operation, and $N_0 = 2\sigma^2$ is the noise power spectral density.

*Proof:* Let us first define $\mathbf{r} = \mathbf{y}/f$ and $\mathbf{v} = \mathbf{w}/f$ for use in the following expressions. The PEP of the supersymbol constellation can be expressed as

$$\mathcal{P}\left(\mathbf{s}_m^k \to \mathbf{s}_n^l\right) = \mathcal{P}\left( \left\| \mathbf{r} - \mathbf{s}_m^k \right\|^2 > \left\| \mathbf{r} - \mathbf{s}_n^l \right\|^2 \right)$$

$$= \mathcal{P}\left( \sum_{i=1}^{N_r} p_{k_i} |b_{m_i}|^2 - 2\mathcal{R}\left\{ r_i^* \sqrt{p_{k_i}} b_{m_i} \right\} \right.$$

$$\left. > \sum_{i=1}^{N_r} p_{l_i} |b_{n_i}|^2 - 2\mathcal{R}\left\{ r_i^* \sqrt{p_{l_i}} b_{n_i} \right\} \right). \tag{21}$$

Since, for PSK signals, we have $|b_{m_i}| = 1$, by rearranging the terms in the probability expression, (21) can be further

358 simplified as

$$\mathcal{P}\left(\mathbf{s}_m^k \to \mathbf{s}_n^l\right) = \mathcal{P}\left(\sum_{i=1}^{N_r} \mathcal{R}\left\{r_i^* \sqrt{p_{l_i}} b_{n_i}\right\} - \mathcal{R}\left\{r_i^* \sqrt{p_{k_i}} b_{m_i}\right\}\right.$$
$$\left. > \frac{\sum_{i=1}^{N_r} p_{l_i} - \sum_{i=1}^{N_r} p_{k_i}}{2}\right). \quad (22)$$

359 Since $\sum_{i=1}^{N_r} p_{l_i} = \sum_{i=1}^{N_r} p_{k_i} = 1$ and $r_i = \sqrt{p_{k_i}} b_{m_i} + v_i$, we
360 have

$$\mathcal{P}\left(\mathbf{s}_m^k \to \mathbf{s}_n^l\right) = \mathcal{P}\left(\sum_{i=1}^{N_r} \mathcal{R}\left\{\sqrt{p_{k_i}} b_{m_i}^* \sqrt{p_{l_i}} b_{n_i}\right\} + \mathcal{R}\left\{v_i^* \sqrt{p_{l_i}} b_{n_i}\right\}\right.$$
$$> \sum_{i=1}^{N_r} p_{k_i} |b_{m_i}|^2 + \mathcal{R}\left\{v_i^* \sqrt{p_{k_i}} b_{m_i}\right\}\right)$$
$$= \mathcal{P}\left(\sum_{i=1}^{N_r} \mathcal{R}\left\{v_i^* (\sqrt{p_{l_i}} b_{n_i} - \sqrt{p_{k_i}} b_{m_i})\right\}\right.$$
$$\left. > 1 - \sum_{i=1}^{N_r} \sqrt{p_{k_i} p_{l_i}} \mathcal{R}\left\{b_{m_i}^* b_{n_i}\right\}\right). \quad (23)$$

361   Let us define the random variable $\chi \hat{=} \sum_{i=1}^{N_r} \mathcal{R}\{v_i^*(\sqrt{p_{l_i}} b_{n_i} - $
362 $\sqrt{p_{k_i}} b_{m_i})\}$ for which we have $\chi \in \mathcal{N}(0, AN_0/f^2)$ with

$$A = \frac{\sum_{i=1}^{N_r} p_{l_i} |b_{n_i}|^2 + p_{k_i} |b_{n_i}|^2}{2} = \frac{1}{2} \sum_{i=1}^{N_r} p_{l_i} + p_{k_i}. \quad (24)$$

363   For the unity transmit power assumed in this paper, it can be
364 seen from (24) that $A = 1$. Accordingly, for the PEP, we have

$$\mathcal{P}\left(\mathbf{s}_m^k \to \mathbf{s}_n^l\right) = \mathcal{P}\left(\chi > 1 - \sum_{i=1}^{N_r} \sqrt{p_{k_i} p_{l_i}} \mathcal{R}\left\{b_{m_i}^* b_{n_i}\right\}\right) \quad (25)$$

365 which, for $\chi \in \mathcal{N}(0, N_0/f^2)$, leads to (20).   ∎

### 366 B. Optimum Power Ratio $\alpha$

367   As mentioned earlier, the power ratio $\alpha$ determines the
368 reliability of detection for the spatial symbol, whereas the lower
369 power level $P_2$ dominates the BER performance of the classic
370 modulated symbols' detection. As the probability of error in
371 (19) is dominated by the maximum PEP, the optimum power
372 ratio should be selected as

$$\alpha_{\mathrm{opt}} = \arg\min_{\alpha} \max_{\mathbf{s}_m^k, \mathbf{s}_n^l} \left\{\mathcal{P}\left(\mathbf{s}_m^k \to \mathbf{s}_n^l\right)\right\}. \quad (26)$$

373   To simplify the analysis, we shall treat the errors in the spatial
374 and classic modulated symbols separately. Accordingly, for the
375 maximum PEP $\mathcal{P}_m(s_{m_i}^k \to s_{m_i}^l)$ in the spatial domain only, we
376 have the following theorem.

377   *Theorem 2:* The maximum PEP $\mathcal{P}_m(s_{m_i}^k \to s_{m_i}^l)$ for the
378 spatial symbols in DLT can be expressed as

$$\mathcal{P}_m\left(s_{m_i}^k \to s_{m_i}^l\right) = Q\left(\frac{f}{\sqrt{N_0}} \cdot \frac{\sqrt{P_2} - \sqrt{P_1}}{2}\right). \quad (27)$$

379   *Proof:* The maximum PEP in the spatial domain involves
380 the adjacent symbols of different power levels in the supersym-
381 bol constellation and can be expressed as

$$\mathcal{P}_m\left(s_{m_i}^k \to s_{m_i}^l\right)$$
$$= \mathcal{P}\left(\left\|r_i - s_{m_i}^k\right\|^2 > \left\|r_i - s_{m_i}^l\right\|^2\right)$$
$$= \mathcal{P}\left(P_1 - 2\mathcal{R}\left\{r_i^* \sqrt{P_1} b_{m_i}\right\} > P_2 - 2\mathcal{R}\left\{r_i^* \sqrt{P_2} b_{m_i}\right\}\right) \quad (28)$$

382 where, using $r_i = \sqrt{p_{k_i}} b_{m_i} + v_i$, we get

$$\mathcal{P}_m\left(s_{m_i}^k \to s_{m_i}^l\right)$$
$$= \mathcal{P}\left(P_1 - 2P_1 |b_{m_i}|^2 - 2\mathcal{R}\left\{u_i^* \sqrt{P_1} b_{m_i}\right\}\right.$$
$$\left. > P_2 - 2\sqrt{P_1 P_2} |b_{m_i}|^2 - 2\mathcal{R}\left\{u_i^* \sqrt{P_2} b_{m_i}\right\}\right)$$
$$= \mathcal{P}\left(2(\sqrt{P_2} - \sqrt{P_1})\mathcal{R}\left\{u_i^* b_{m_i}\right\} > P_1 + P_2 - 2\sqrt{P_1 P_2}\right)$$
$$= \mathcal{P}\left(-\mathcal{R}\left\{u_i^* b_{m_i}\right\} > \frac{\sqrt{P_1} - \sqrt{P_2}}{2}\right). \quad (29)$$

383   Similarly to the given proof, we have used the fact
384 that $|b_{m_i}|^2 = 1$, and it can be seen that $\psi \hat{=} - \mathcal{R}\{u_i^* b_{m_i}\} \in$
385 $\mathcal{N}(0, N_0/f^2)$. Accordingly, for the minimum PEP in the spatial
386 constellation, we have

$$\mathcal{P}_m\left(s_{m_i}^k \to s_{m_i}^l\right) = \mathcal{P}\left(\psi > \frac{\sqrt{P_2} - \sqrt{P_1}}{2}\right) \quad (30)$$

387 which leads to (27).   ∎
  This indicates that the separation between $\{P_1, P_2\}$ should
388 be maximized for minimizing the errors in the spatial bits,
389 which are dominated by the distance between the pairs of adja-
390 cent symbols having different power levels $d_s = \sqrt{P_1} - \sqrt{P_2}$.
391 We therefore define the spatial function $f_S(\alpha)$ that accounts for
392 the dependence of the spatial errors on $\alpha$ as

$$f_S(\alpha) \triangleq \sqrt{P_1} - \sqrt{P_2} = \frac{1 - \sqrt{\alpha}}{\sqrt{(N_r - N_a)\alpha + N_a}}. \quad (31)$$

394   As regards to the classic modulated symbol errors, it is
395 known that the PSK error probability is given as [41]

$$\mathcal{P}\left(s_{m_i}^k \to s_{n_i}^k\right) = \mathcal{P}\left(\left\|r_i - s_{m_i}^k\right\|^2 > \left\|r_i - s_{n_i}^l\right\|^2\right)$$
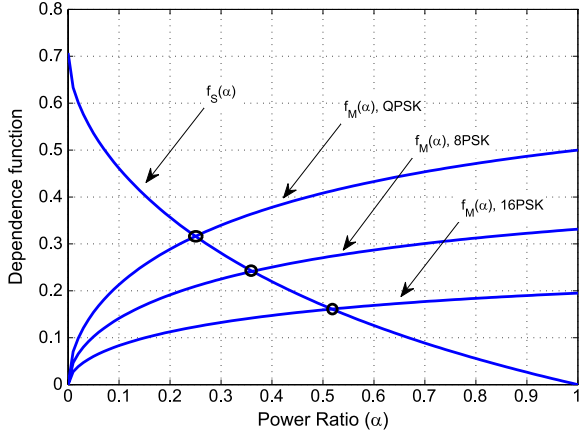$$= Q\left(f\sqrt{\frac{P_2}{N_0} \log_2(M)} \sin\frac{\pi}{M}\right). \quad (32)$$

Fig. 4. Theoretical optimization of $\alpha$ for DLT for a $(8 \times 4)$ MIMO with $N_a = 2$, using (36).

TABLE II
COMPLEXITY FOR SMX, RSM, AND THE PROPOSED DLT SCHEME.
$N_\chi = N_a$ FOR RSM, $N_\chi = N_r$ FOR DLT

|  | Operations |
| --- | --- |
| *Transmitter:* |  |
| ZF processing | $N_r^3 + 2N_t N_r$ |
| *Receiver:* |  |
| Spatial detection | $2N_a \binom{N_r}{N_a}$ |
| Demodulation | $N_\chi M$ |
| **SMX Total** | $C_{SMX} = N_r^3 + N_r(2N_t + M)$ |
| **RSM Total** | $C_{RSM} = N_r^3 + 2N_t N_r + N_a \left( 2\binom{N_r}{N_a} + M \right)$ |
| **DLT Total** | $C_{DLT} = N_r^3 + N_r(2N_t + M) + 2N_a \binom{N_r}{N_a}$ |

Accordingly, we define the function $f_M(\alpha)$ for the dependence of the modulated symbol error on $\alpha$ as

$$f_M(\alpha) \triangleq \sqrt{P_2 \log_2(M) \sin \frac{\pi}{M}}$$
$$= \sqrt{\log_2(M) \sin \frac{\pi}{M} \cdot \frac{\alpha}{(N_r - N_a)\alpha + N_a}}. \quad (33)$$

The optimization (26) is equivalent to the maximization of the minimum of these functions:

$$\alpha_{\text{opt}} = \arg \max_\alpha \left\{ \min \left\{ f_S(\alpha), f_M(\alpha) \right\} \right\}. \quad (34)$$

The optimum power scaling ratio is, therefore, given as

$$\alpha_{\text{opt}} = \arg \max_\alpha \left\{ \frac{1 - \sqrt{\alpha}}{\sqrt{(N_r - N_a)\alpha + N_a}}, \right.$$
$$\left. \sqrt{\log_2(M) \sin \frac{\pi}{M} \cdot \frac{\alpha}{(N_r - N_a)\alpha + N_a}} \right\} \quad (35)$$

which is equivalent to selecting the factor $\alpha$ so that the two terms in the minimization become equal, which gives

$$\alpha_{\text{opt}} = \frac{1}{\left( 1 + \sqrt{\log_2(M) \sin \frac{\pi}{M}} \right)^2}. \quad (36)$$

We examine this optimization in Fig. 4, which shows the functions $f_s(\alpha), f_M(\alpha)$ when increasing the values of $\alpha$ for the example of a $(8 \times 4)$-element DLT system with $N_a = 2$, for $M = 4, 8, 16$, i.e., quadrature phase-shift keying (QPSK), 8PSK, and 16PSK modulation. The intersections of the lines determine the optimum values of $\alpha$. It will be shown in the following that the theoretically obtained optimal values of $\alpha$ closely match the optimal values obtained by simulation.

## V. COMPLEXITY AND POWER EFFICIENCY

### A. Complexity

Here, we compare the computational complexity of SMX, RSM, and DLT and use this to carry out a comparison of the resulting PE of the techniques. First, Table II summarizes the computational complexity of each of the techniques, taking into account the dominant operations at the transmitter and receiver. We follow the typical assumption that multiplications and additions require an equal number of floating point operations. For all three schemes, the ZF-TPC employed at the transmitter involves the inversion of the channel matrix that requires $N_r^3 + N_t N_r$ operations and the multiplication with the supersymbol vector involving an additional $N_t N_r$ operations. At the receiver, all techniques require a demodulation stage that involves $M$ comparisons for and $M$-order modulation, for each antenna receiving information, i.e., $N_r M$ for both SMX and DLT, and $N_a M$ for RSM. The RSM and DLT require an additional stage for the detection of the spatial symbol which, from (6) involves $N_a$ complex multiplications and $N_a$ complex additions for each antenna combination out of the $\binom{N_r}{N_a}$ combinations in total.

### B. Power Efficiency

As the ultimate metric for evaluating the performance–complexity tradeoff and the overall usefulness of the proposed technique, we consider the PE of DLT compared with SMX and RSM. Following the modeling of [43]–[46], we define the PE of the communication link as the bit rate per total transmit power dissipated, i.e., the ratio of the goodput achieved over the power consumed:

$$\mathcal{E} = \frac{T}{P_{\text{PA}} + N_t \cdot P_t^{\text{RF}} + N_r \cdot P_r^{\text{RF}} + p_c \cdot C} \quad (37)$$

where $P_{\text{PA}} = ((\xi/\eta) - 1)P$ in Watts is the power dissipated by the power amplifier to produce the total transmit signal power $P$, with $\eta$ being the power amplifier's efficiency and $\xi$ being the modulation-dependent peak-to-average power ratio (PAPR). Furthermore, $P_t^{\text{RF}} = P_{\text{mix}} + P_{\text{filt}} + P_{\text{DAC}}$ and $P_r^{\text{RF}} = P_{\text{mix}} + P_{\text{filt}} + P_{\text{ADC}}$ represent the RF powers related to the mixers, to the transmit filters, to the digital-to-analog converter (DAC) at the transmitter and to the analog-to-digital converter (ADC) at the receiver, which are assumed to be constant for the purposes of this paper. We use practical values of these from [44] as $\eta = 0.35$ and $P_{\text{mix}} = 30.3$ mW, $P_{\text{filt}} = 2.5$ mW, $P_{\text{DAC}} = 1.6$ mW, and $P_{\text{DAC}} = 1.3$ mW, yielding $P_t^{\text{RF}} = 34.4$ mW, and $P_r^{\text{RF}} = 34.1$ mW. In (37), $p_c$ in Watts/KOps is the power per $10^3$ elementary

operations (KOps) of the digital signal processor, and $C$ is the number of operations involved, taken from Table II, where it is assumed that the operations shown dominate the digital signal processing complexity of the link. This term is used for introducing the complexity as a factor related to the power dissipation in the PE metric. Typical values of $p_c$ include $p_c = 22.88$ mW/KOps for the Virtex-4 and $p_c = 5.76$ mW/KOps for the Virtex-5 FPGA family from Xilinx [47]. Finally

$$T = \beta B(1 - P_B) = \beta B(1 - P_e)^B \qquad (38)$$

represents the achieved goodput, where $P_B$ is the block error rate with a block of size $B$ symbols, and $\beta$ is the BE of SM in bits per symbol, taken from Table I. For reference, we have assumed an LTE Type-2 TDD frame structure [48]. This has a 10 ms duration that consists of 10 subframes, out of which five subframes, containing 14 symbol time slots each, are used for DL transmission yielding a block size of $B = 70$ for the DL, whereas the remainder are used for both uplink (UL) and control information transmission. A slow fading channel is assumed where the channel remains constant for the duration of the frame.

The expression in (37) provides an amalgamated metric that combines goodput, complexity, and transmit signal power, all in a unified metric. High values of $\mathcal{E}$ indicate that high bit rates are achievable for a given power consumption and thus denote high energy efficiency. The following results show that DLT provides an increased energy efficiency compared with SMX and RSM in numerous scenarios using different transmit power levels $P$.

## VI. NUMERICAL RESULTS

To evaluate the benefits of the proposed technique, this section presents numerical results based on Monte Carlo simulations of SMX, RSM, and the proposed DLT. The channel impulse response is assumed perfectly known at the transmitter. Without loss of generality, unless stated otherwise, we assume that the transmit power is restricted to $P = 1$. MIMO systems with up to eight TAs employing QPSK and 8PSK modulation are explored, albeit it is plausible that the benefits of the proposed technique extend to larger scale systems and higher order modulation.

*Remark:* It should be noted that the BE improvement shown in the following could also be obtained by SMX with the aid of an increased classical modulation order. Accordingly, in the following, we compare the proposed DLT to: (a) SMX using the same classical modulation order to illustrate the improved BE of DLT; and (b) SMX relying on a higher modulation order to highlight the improved performance of DLT for an identical BE.

In Fig. 5, we show the BER as a function of the power ratio for DLT for the $(8 \times 4)$ MIMO system, where the values of $\alpha$ in the area of 0.25 can be seen to provide the best performance. This matches well with the theoretically derived result of Section IV-A and Fig. 4. Similarly, Fig. 6 shows the BER versus $\alpha$ performance for higher order modulation 8PSK and 16PSK. Again, a close match can be seen with the theoretically derived values for $\alpha_{\text{opt}}$. In Fig. 7, we show the BER with increasing SNR for the proposed DLT, where the black
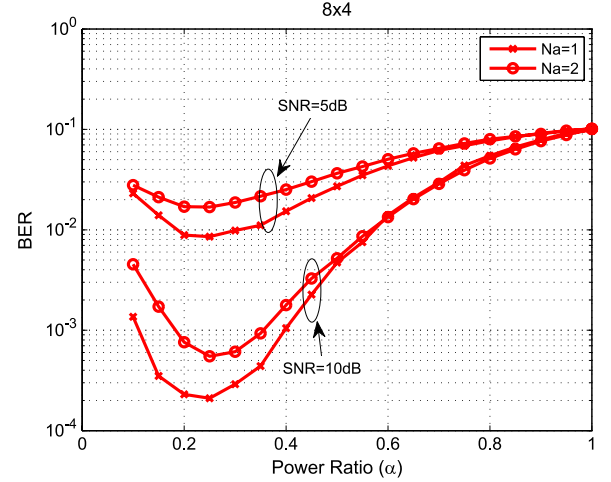


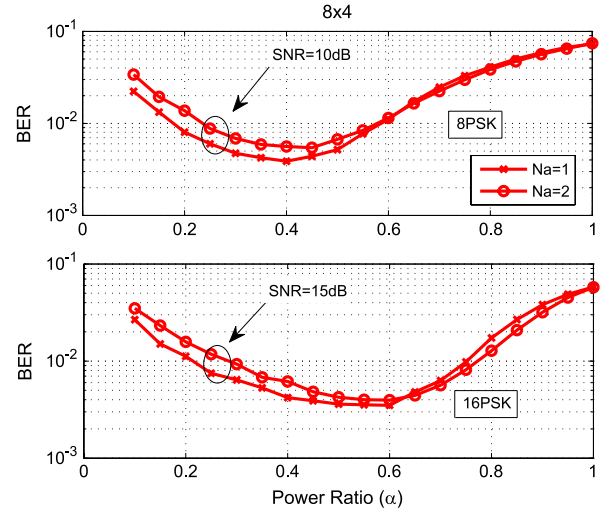Fig. 5. BER versus $\alpha$ for an $(8 \times 4)$ MIMO with SMX and DLT, as well as QPSK with Rayleigh fading.



Fig. 6. BER versus $\alpha$ for a $(8 \times 4)$ MIMO with DLT, as well as 8PSK and 16PSK with Rayleigh fading.
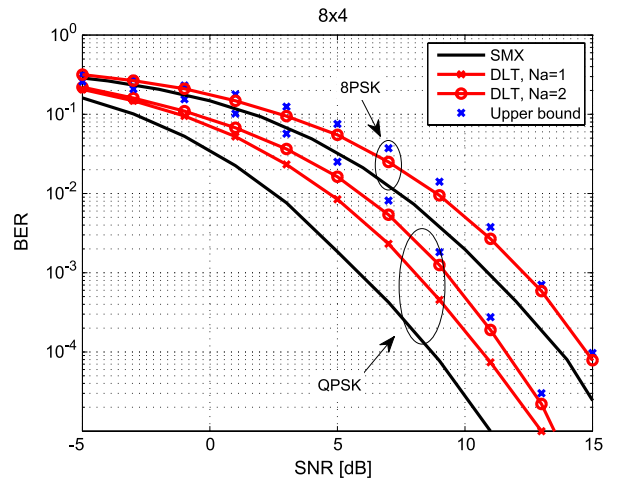


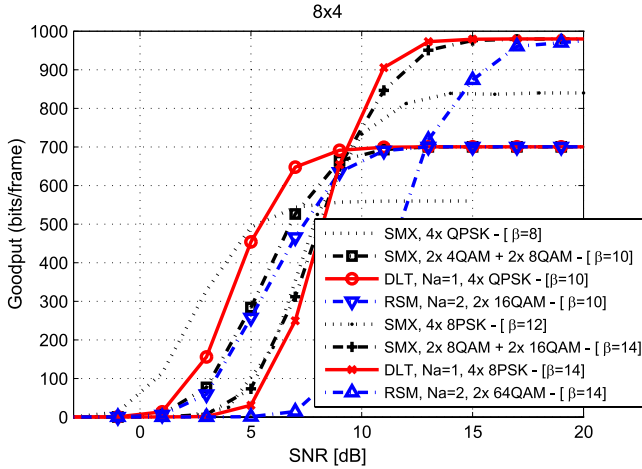Fig. 7. BER versus SNR for a $(8 \times 4)$ MIMO with SMX and DLT, as well as QPSK and 8PSK with Rayleigh fading.

Fig. 8. Goodput versus SNR for a $(8 \times 4)$ MIMO with SMX and DLT, as well as Rayleigh fading.
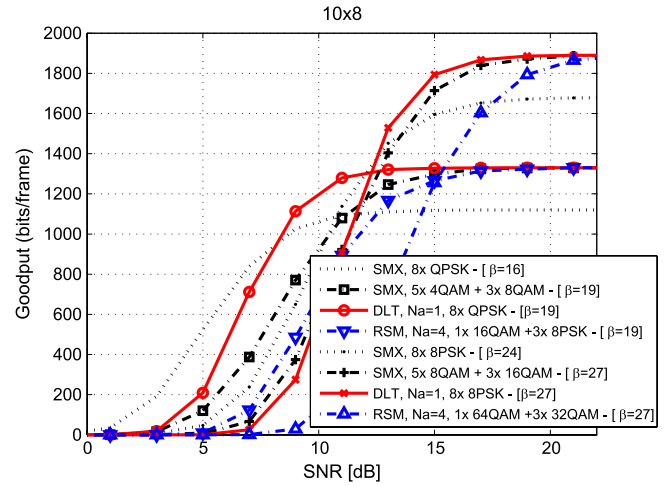


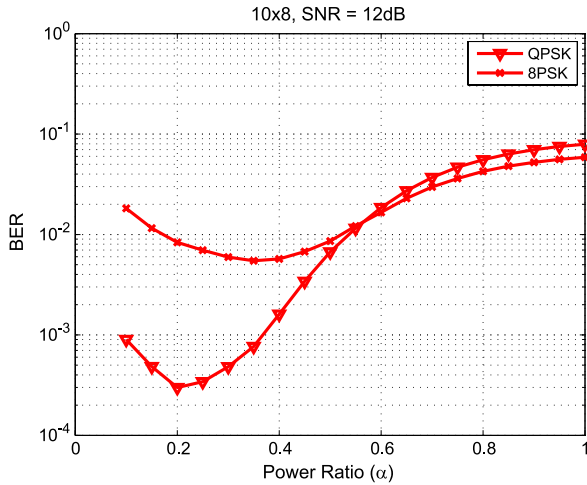Fig. 10. Goodput versus SNR for a $(10 \times 8)$ MIMO with SMX and DLT, as well as Rayleigh fading.



Fig. 9. BER versus $\alpha$ for a $(10 \times 8)$ MIMO with DLT, QPSK, and 8PSK with Rayleigh fading.
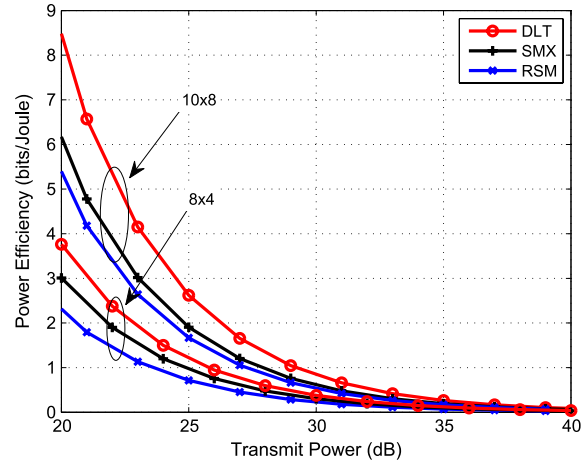


Fig. 11. PE versus transmit power for $(10 \times 8)$ and $(8 \times 4)$ MIMO systems with SMX and DLT, as well as QPSK with Rayleigh fading.

lines for $N_a = 4$ represent SMX transmission. The curves show results for both QPSK and 8PSK. The theoretical upper bound using (19) is also depicted for both cases, and it can be observed that it offers a tight bound. Clearly, the DLT scheme has inferior BER performance compared with SMX due to the additional spatial streams but at the benefit of improved BE. The improved BE of DLT is demonstrated in Fig. 8 where the goodput with increasing SNR is depicted for the same $(8 \times 4)$ MIMO scenario. Clearly, DLT provides higher goodput than SMX for sufficiently high SNR values. To complete our comparisons, for both scenarios in the figure, we also show the cases where the symbol modulation order used for SMX and RSM is increased for some of the spatial streams in order to achieve the same BE values of $\beta = 10$ and $\beta = 14$ with the proposed DLT, for QPSK and 8PSK, respectively. Clearly, this has an impact on the SNR requirement of SMX, where it can be seen that the proposed DLT scheme obtains the maximum goodput at lower SNR values.

The performance comparison is extended to the $(10 \times 8)$ MIMO system in Figs. 9 and 10. In Fig. 9, we show the

BER as a function of the power ratio for DLT, where the best performance is provided for $\alpha$ in the range of 0.2 for QPSK and 0.4 for 8PSK. Fig. 10 shows the goodput with increasing SNR, where again it can be observed that the DLT provides better goodput than SMX at higher SNR values. As above, for both scenarios characterized in the figure, we also include the cases where the symbol modulation order used for SMX and RSM is increased for some of the spatial streams in order to achieve the same BE values of $\beta = 19$ and $\beta = 27$ with the proposed DLT, for QPSK and 8PSK, respectively. Again, it can be seen that the proposed DLT scheme obtains the maximum goodput at lower SNR values.

Finally, Figs. 11 and 12 show the PE of the SMX, RSM and DLT techniques. Fig. 11 shows the PE for increasing transmit power, within the region of power values used in the communication standards for $(10 \times 8)$ and $(8 \times 4)$ MIMO systems. It is assumed here that the noise variance is $\sigma^2 = 1$ to indirectly account for the path loss (and, hence, the useful signal power loss) experienced in real transmission. It can be seen that the proposed DLT scheme outperforms SMX and RSM in terms
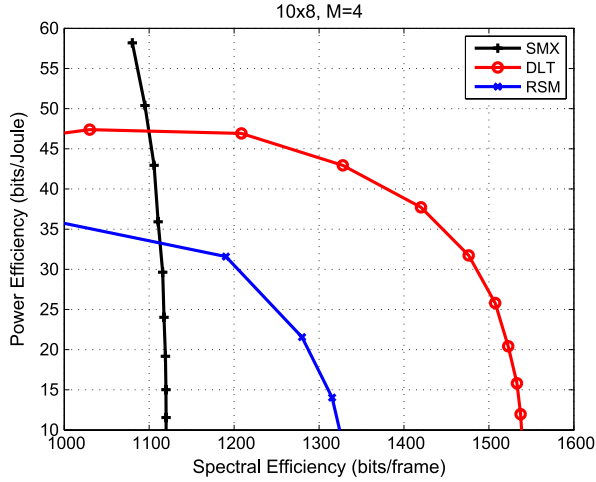
Fig. 12. Power efficiency versus spectral efficiency for a $(10 \times 8)$ MIMO with SMX and DLT, as well as QPSK with Rayleigh fading.

547 of PE for all transmit power values in both $(10 \times 8)$ and $(8 \times 4)$
548 MIMO systems. The tradeoff between PE and BE is shown in
549 Fig. 12. It can be seen that DLT offers a more scalable tradeoff
550 with a wider range of BEs for the PE range, while it is more
551 power efficient than SMX and RSM in the region of high BEs.

## VII. CONCLUSION

553    A dual-layered DL transmission scheme was proposed,
554 which combines traditional MIMO SMX with RSM. As op-
555 posed to traditional SM where a subset of antennas carry a spa-
556 tial stream, here, we allow all antennas to carry information by
557 applying SM on the symbol power-level domain. This provides
558 scope for the analytical optimization of the ratio between the
559 power levels used in the proposed scheme. Both our simulations
560 and performance analysis show that, by allowing all antennas
561 to form spatial streams, the proposed scheme improves the
562 system's BE and power efficiency compared to both SMX
563 and SM.
564    Further work can involve exploring more advanced TPC
565 schemes for the proposed transmission scheme and exploring
566 the adaptations of the proposed scheme for QAM and enhanc-
567 ing its robustness to channel state information errors.

## REFERENCES

[1] D. Gesbert, M. Kountouris, R. Heath, C. Chae, and T. Salzer, "Shifting the MIMO paradigm," *IEEE Signal Process. Mag.*, vol. 24, no. 5, pp. 36–46, Sep. 2007.
[2] M. Costa, "Writing on dirty paper," *IEEE Trans. Inf. Theory*, vol. IT-29, no. 3, pp. 439–441, May 1983.
[3] C. Windpassinger, R. Fischer, T. Vencel, and J. Huber, "Precoding in multi-antenna and multiuser communications," *IEEE Trans. Wireless Commun.*, vol. 3, no. 4, pp. 1305–1316, Jul. 2004.
[4] C. Masouros, M. Sellathurai, and T. Rantarajah, "Interference optimiza-tion for transmit power reduction in Tomlinson–Harashima precoded MIMO downlinks," *IEEE Trans. Signal Process.*, vol. 60, no. 5, pp. 2470–2481, May 2012.
[5] A. Garcia and C. Masouros, "Power loss reduction for MMSE-THP with multidimensional symbol scaling," *IEEE Commun. Lett.*, vol. 18, no. 7, pp. 1147–1150, Jul. 2014.
[6] A. Garcia and C. Masouros, "Power-efficient Tomlinson–Harashima precoding for the downlink of multi-user MISO systems," *IEEE Trans. Commun.*, vol. 62, no. 6, pp. 1884–1896, Jun. 2014.
[7] C. B. Peel, B. M. Hochwald, and A. L. Swindlehurst, "A vector-perturbation technique for near-capacity multiantenna multiuser communication—Part I: Channel inversion and regularization," *IEEE Trans. Commun.*, vol. 53, no. 1, pp. 195–202, Jan. 2005.
[8] C. Masouros and E. Alsusa, "Dynamic linear precoding for the exploita-tion of known interference in MIMO broadcast systems," *IEEE Trans. Wireless Commun.*, vol 8, no. 3, pp. 1396–1404, Mar. 2009.
[9] C. Masouros and E. Alsusa, "Soft transmitter precoding for the down-link of DS/CDMA communication systems," *IEEE Trans. Veh. Technol.*, vol. 59, no. 1, pp. 203–215, Jan. 2010.
[10] C. Masouros, T. Ratnarajah, M. Sellathurai, C. Papadias, and A. Shukla, "Known interference in wireless communications: A limiting factor or a potential source of green signal power?" *IEEE Commun., Mag.*, vol. 51, no. 10, pp. 162–171, Oct. 2013.
[11] G. Zheng *et al.*, "Rethinking the role of interference in wireless networks," *IEEE Commun. Mag.*, vol. 52, no. 11, pp. 152,158, Nov. 2014.
[12] C. Masouros, "Correlation rotation linear precoding for MIMO broadcast communications," *IEEE Trans. Signal Process.*, vol 59, no. 1, pp. 252–262, Jan. 2011.
[13] F. Rusek *et al.*, "Scaling up MIMO: Opportunities and challenges with very large arrays," *IEEE Signal Process. Mag.*, vol. 30, no. 1, pp. 40–60, Jan. 2013.
[14] C. Masouros, M. Sellathurai, and T. Ratnarajah, "Large-scale MIMO transmitters in fixed physical spaces: The effect of transmit correlation and mutual coupling," *IEEE Trans. Commun.*, vol. 61, no. 7, pp. 2794–2804, Jul. 2013.
[15] C. Masouros and M. Matthaiou, "Physically constrained massive MIMO: Hitting the wall of favorable propagation," *IEEE Commun. Let.*, vol. 19, no. 5, pp. 771–774, May 2015.
[16] R. Mesleh, H. Haas, S. Sinanovic, C. W. Ahn, and S. Yun, "Spatial modulation," *IEEE Trans. Veh. Technol.*, vol. 57, no. 4, pp. 2228–2241, Jul. 2008.
[17] M. Di Renzo, H. Haas, A. Ghrayeb, S. Sugiura, and L. Hanzo, "Spatial modulation for generalized MIMO: Challenges, opportunities, and imple-mentation," *Proc. IEEE*, vol. 102, no. 1, pp. 56–103, Jan. 2014.
[18] A. Garcia and C. Masouros, "Low-complexity compressive sensing detec-tion for spatial modulation in large-scale multiple access channels," *IEEE Trans. Commun.*, to be published.
[19] M. Di Renzo and H. Haas, "Bit error probability of space modulation over Nakagami-m fading: Asymptotic analysis," *IEEE Commun. Lett.*, vol. 15, no. 10, pp. 1026–1028, Oct. 2011.
[20] J. Jeganathan, A. Ghrayeb, and L. Szczecinski, "Spatial modulation: Optimal detection and performance analysis," *IEEE Commun. Lett.*, vol. 12, no. 8, pp. 545–547, Aug. 2008.
[21] A. Younis, S. Sinanovic, M. Di Renzo, R. Mesleh, and H. Haas, "Gen-eralised sphere decoding for spatial modulation," *IEEE Trans. Commun.*, vol. 61, no. 7, pp. 2805–2815, Jul. 2013.
[22] J. Wang, S. Jia, and J. Song, "Generalised spatial modulation system with multiple active transmit antennas and low complexity detection scheme," *IEEE Trans. Wireless Commun.*, vol. 11, no. 4, pp. 1605–1615, Apr. 2012.
[23] M. Di Renzo and H. Haas, "On transmit diversity for spatial modulation MIMO: Impact of spatial constellation diagram and shaping filters at the transmitter," *IEEE Trans. Veh. Technol.*, vol. 62, no. 6, pp. 2507–2531, Jul. 2013.
[24] P. Yang *et al.*, "Star-QAM signaling constellations for spatial mod-ulation," *IEEE Trans. Veh. Technol.*, vol. 63, no. 8, pp. 3741–3749, Oct. 2014.
[25] S. Sugiura, C. Xu, S. X. Ng, and L. Hanzo, "Reduced-complexity coherent versus non-coherent QAM-aided space-time shift keying," *IEEE Trans. Commun.*, vol. 59, no. 11, pp. 3090–3101, Nov. 2011.
[26] K. Ntontin, M. Di Renzo, A. Perez-Neira, and C. Verikoukis, "Adaptive generalized space shift keying," *EURASIP J. Wireless Commun. Netw.*, vol. 2013, no. 1, p. 43, Feb. 2013.
[27] S. Sugiura and L. Hanzo, "On the joint optimization of dispersion matrices and constellations for near-capacity irregular precoded space-time shift keying," *IEEE Trans. Wireless Commun.*, 2013, vol. 12, no. 1, pp. 380–387, Jan. 2013.
[28] M. Maleki, H. Bahrami, S. Beygi, M. Kafashan, and N. H. Tran, "Space modulation with CSI: Constellation design and performance evaluation," *IEEE Trans. Veh. Technol.*, vol. 62, no. 4, pp. 1623–1634, May 2013.
[29] X. Guan, Y. Cai, and W. Yang, "On the mutual information and precoding for spatial modulation with finite alphabet," *IEEE Wireless Commun. Lett.*, vol. 2, no. 4, pp. 383–386, Aug. 2013.

AQ1

[30] J. M. Luna-Rivera, D. U. Campos-Delgado, and M. G. Gonzalez-Perez, "Constellation design for spatial modulation," *Procedia Technol.*, vol. 7, pp. 71–78, 2013.

[31] C. Masouros, "Improving the diversity of spatial modulation in MISO channels by phase alignment," *IEEE Commun. Lett.*, vol. 18, no. 5, pp. 729–732, May 2014.

[32] A. Garcia, C. Masouros, and L. Hanzo, "Pre-scaling optimization for space shift keying based on semidefinite relaxation," *IEEE Trans. Commun.*, to be published.

[33] C. Masouros and L. Hanzo, "Constellation-randomization achieves transmit diversity for single-RF spatial modulation," *IEEE Trans. Veh. Technol.*, to be published.

[34] J. Jeganathan, A. Ghrayeb, L. Szczecinski, and A. Ceron, "Space shift keying modulation for MIMO channels," *IEEE Trans. Wireless Commun.*, vol. 8, no. 7, pp. 3692–3703, Jul. 2009.

[35] M. Di Renzo and H. Haas, "Bit error probability of space modulation over Nakagami-m fading: Asymptotic analysis," *IEEE Commun. Lett.*, vol. 15, no. 10, pp. 1026–1028, Oct. 2011.

[36] R. Zhang, L. Yang, and L. Hanzo, "Generalised pre-coding aided spatial modulation," *IEEE Trans. Wireless Commun.,* vol. 12, no. 11, pp. 5434–5443, Nov. 2013.

[37] D.-T. Phan-Huy and M. Helard, "Receive antenna shift keying for time reversal wireless communications," in *Proc. IEEE ICC*, Jun. 2012, pp. 4852–4856.

[38] R. Zhang, L. L. Yang, and L. Hanzo, "Error probability and capacity analysis of generalised pre-coding aided spatial modulation," *IEEE Trans. Wireless Commun.*, vol. 14, no. 1, pp. 364–375, Jan. 2015.

[39] A. Stavridis, S. Sinanovic, M. Di Renzo, and H. Haas, "Transmit precoding for receive spatial modulation using imperfect channel knowledge," in *Proc. IEEE Veh. Technol. Conf. Spring*, May 2012, pp. 1–5.

[40] R. M. Legnain, R. H. M. Hafez, I. D. Marsland, and A. M. Legnain, "A novel spatial modulation using MIMO spatial multiplexing," in *Proc. ICCSPA*, Feb. 2013, pp. 1–4.

[41] J. G. Proakis, *Digital Communications*, Electrical Engineering, 3rd ed. New York, NY, USA: McGraw-Hill, 1995.

[42] M. Abramowitz and I. A. Stegun, *Handbook of Mathematical Functions With Formulas, Graphs, and Mathematical Tables.* New York, NY, USA: Dover, 1972.

[43] X. Cong, G. Y. Li, Z. Shunqing, Y. Chen, and S. Xu, "Energy- and spectral-efficiency tradeoff in downlink OFDMA networks," *IEEE Trans. Wireless Commun.*, vol. 10, no. 11, pp. 3874–3886, Nov. 2011.

[44] S. Cui, A. J. Goldsmith, and A. Bahai, "Energy-constrained modulation optimization," *IEEE Trans. Wireless Commun.*, vol. 4, no. 5, pp. 2349–2360, Sep. 2005.

[45] C. Masouros, M. Sellathurai, and T. Ratnarajah, "Computationally efficient vector perturbation precoding using thresholded optimization," *IEEE Trans. Commun.*, vol. 61, no. 5, pp. 1880–1890, May 2013.

[46] C. Masouros, M. Sellathurai, and T. Ratnarajah, "Vector perturbation based on symbol scaling for limited feedback MIMO downlinks," *IEEE Trans. Signal Process.*, vol. 62, no. 3, pp. 562–571, Feb. 1, 2014.

[47] D. Curd, Power consumption in 65 nm FPGAs, Xilinx White Paper, Feb. 2007.

[48] *Evolved Universal Terrestrial Radio Access (E-UTRA); LTE Physical Layer; General Description*, Third-Generation Partnership Project, TS 36.201, V11.1.0 (2008-03), Rel. 11, 2008.

**Christos Masouros** (M'06–SM'14) received the Diploma in electrical and computer engineering from the University of Patras, Patras, Greece, in 2004 and the M.Sc. and Ph.D. degrees in electrical and electronic engineering from The University of Manchester, Manchester, U.K., in 2006 and 2009, respectively.

He was a Research Associate with the University of Manchester and a Research Fellow with Queen's University Belfast, Belfast, U.K. He is currently a Lecturer with the Department of Electrical and Electronic Engineering, University College London, London, U.K. His research interests include wireless communications and signal processing, with particular focus on green communications, large-scale antenna systems, cognitive radio, and interference mitigation techniques for multiple-input–multiple-output and multicarrier communications.

Dr. Masouros is the Principal Investigator of the EPSRC Project EP/M014150/1 on large-scale antenna systems. He received a Royal Academy of Engineering Research Fellowship for 2011–2016.

**Lajos Hanzo** (M'91–SM'92–F'04) received the M.S. degree in electronics and the Ph.D. degree from Budapest University of Technology and Economics (formerly, Technical University of Budapest), Budapest, Hungary, in 1976 and 1983, respectively; the D.Sc. degree from the University of Southampton, Southampton, U.K., in 2004; and the "Doctor Honoris Causa" degree from Budapest University of Technology and Economics in 2009.

During his 38-year career in telecommunications, he has held various research and academic posts in Hungary, Germany, and the U.K. Since 1986, he has been with the School of Electronics and Computer Science, University of Southampton, where he holds the Chair in Telecommunications. He is currently directing a 100-strong academic research team, working on a range of research projects in the field of wireless multimedia communications sponsored by industry, the Engineering and Physical Sciences Research Council of U.K., the European Research Council's Advanced Fellow Grant, and the Royal Society Wolfson Research Merit Award. During 2008–2012, he was a Chaired Professor with Tsinghua University, Beijing, China. He is an enthusiastic supporter of industrial and academic liaison and offers a range of industrial courses. He has successfully supervised more than 80 Ph.D. students, coauthored 20 John Wiley/IEEE Press books on mobile radio communications, totaling in excess of 10 000 pages, and published more than 1400 research entries on IEEEXplore. He has more than 20 000 citations. His research is funded by the European Research Council's Senior Research Fellow Grant.

Dr. Hanzo is a Fellow of the Royal Academy of Engineering, The Institution of Engineering and Technology, and the European Association for Signal Processing. He is also a Governor of the IEEE Vehicular Technology Society. He has served as the Technical Program Committee Chair and the General Chair of IEEE conferences, has presented keynote lectures, and has been awarded a number of distinctions. During 2008–2012, he was the Editor-in-Chief of the IEEE Press.

# AUTHOR QUERIES

# Dual-Layered MIMO Transmission for Increased Bandwidth Efficiency

Christos Masouros, *Senior Member, IEEE*, and Lajos Hanzo, *Fellow, IEEE*

*Abstract*—A dual-layered downlink transmission scheme is proposed for intrinsically amalgamating multiple-input–multiple-output (MIMO) spatial multiplexing (SMX) with spatial modulation (SM). The proposed scheme employs a classic SMX transmission that is known to offer superior bandwidth efficiency (BE) compared with SM. We exploit receive-antenna-based SM (RSM) on top of this transmission as an enhancement of the BE. The RSM here is applied to the combined spatial and power-level domain not by activating and deactivating the RAs but rather by choosing between two power levels $\{P_1, P_2\}$ for the received symbols in these antennas. In other words, the combination of symbols received at a power level $P_1$ carries information in the spatial domain in the same manner as the combination of nonzero elements in the receive symbol vector carries information in the RSM transmission. This allows for the coexistence of RSM with SMX, and the results show increased BE for the proposed scheme compared with both SMX and SM. To characterize the proposed scheme, we carry out a mathematical analysis of its performance, and we use this to optimize the ratio between $P_1$ and $P_2$ for attaining the minimum error rates. Our analytical and simulation results demonstrate significant BE gains for the proposed scheme compared with conventional SMX and SM.

*Index Terms*—Multiple-input–multiple-output systems, spatial modulation (SM), spatial multiplexing (SMX), transmit precoding (TPC).

## I. INTRODUCTION

**M**ULTIANTENNA-aided transceivers have been shown to improve the capacity of the wireless channel by means of spatial multiplexing (SMX) [1]. For the multiuser downlink (DL), transmit precoding (TPC) schemes have been shown to improve both the attainable power efficiency (PE) and the cost of mobile terminals by shifting the signal processing complexity to the base stations (BSs). Numerous TPC solutions

exist, ranging from highly complex capacity achieving nonlinear dirty paper coding techniques [2] and their low-complexity suboptimal counterparts in the form of Tomlinson–Harashima precoding [3]–[6] to linear TPC schemes based on channel inversion [7]–[12] that offers the lowest complexity, albeit at an inferior performance. The performance–complexity tradeoffs between the above TPC have been thoroughly studied in the literature. More recently, it has been shown that the family of linear techniques exhibits a close-to-optimal performance in the large-scale multiple-input–multiple-output (MIMO) region [13]–[15]. Accordingly, we focus on the class of low-complexity closed-form linear TPC [7]–[12] due to their favorable performance–complexity tradeoff and practical relevance.

More recently, spatial modulation (SM) has been conceived for implicitly encoding information in the index of the specific antenna activated for the transmission of the modulated symbols, offering a low-complexity design alternative [16]. Its central benefits include the absence of interantenna interference (IAI) and the fact that it only requires a subset (down to one) of radio-frequency (RF) chains compared with SMX. Accordingly, the interantenna synchronization is also relaxed. Early work has focused on the design of receiver algorithms for minimizing the bit error ratio (BER) of SM at low complexity [16]–[21]. The work spans from matched filtering as a low-complexity technique for detecting the antenna index used for SM [16] to the maximum likelihood (ML) [20] with a significantly reduced complexity compared with classic SMX ML detectors, including compressive sensing approaches [18] and performance analyses [19]. Reduced-space sphere detection has also been proposed for SM in [21] for further complexity reduction where a generalized SM transmission was also explored [22]. In addition to receive processing, recent work has also proposed constellation shaping for SM [23]–[33]. Specifically, the work on this topic has focused on three main directions: shaping and optimization of the spatial constellation, i.e., the legitimate sets of activated transmit antennas (TAs) [23], modulation constellation shaping [24]–[28] for the SM and space shift keying transmission, where the constellation of the modulated bits is optimized, and joint spatial and modulation constellation shaping, in the form of optimizing the received constellation [29]–[33].

Closely related work has focused on applying the concept of SM to the receive antennas (RAs) of the communication link, as opposed to the TAs as per the above approaches, forming the RA-based spatial modulation (RSM) concept [36]–[39]. By means of TPC, this technique targets a specific subset of RAs, which receive information symbols, whereas the rest of the RAs

receive only noise. This may be achieved by using zero-forcing (ZF) TPC and transmitting a combination of information symbols and zeros to the RAs, depending on the spatial symbols to convey. As opposed to conventional SM where a subset of RF chains is deployed, here, all TAs and RAs are active and therefore there are no RF chain reductions. Still, the computational complexity of the receivers is drastically reduced, where simply the indexes of the targeted RAs have to be detected, and the classic symbols received at the activated RAs are then demodulated.

Inspired by the above RSM philosophy, here, we propose a dual-layered transmission (DLT) scheme, which intrinsically amalgamates a full spatial multiplexing (SMX) with SM. First, we note that since, for RSM, all TAs and RAs are active, there are no RF chain reductions, and this motivates the full SMX approach. To accommodate the SMX, we apply an SM to the combined spatial and receive-power domain, where instead of sending a combination of information symbols and zero power to the RAs, we apply two different power levels for distinguishing between the "active" and "inactive" RAs. In this manner, the spatial symbols are formed based on the power levels detected. We demonstrate that this improves the bandwidth efficiency (BE) with respect to SMX and SM. Against this state of the art, we list the main contributions of this paper.

- We propose a new DLT scheme based on linear TPC that improves the BE by jointly exploiting the benefits of SMX and RSM.
- We provide the performance analysis of the proposed technique based on the pairwise error probability (PEP) between different constellation points in the supersymbol constellation formed by the combination of the spatial constellation of RSM and the classic modulation constellation of SMX.
- We use the above results for analytically deriving the optimum power ratio between the two sets of antennas that carry the spatial symbol for the proposed scheme for minimizing the probability of detection errors.
- We calculate and compare analytically the complexity of the conventional and proposed techniques, and quantify the performance–complexity tradeoff of conventional and proposed schemes, by introducing a PE metric that combines the BE, transmit power, and complexity, to prove the enhanced tradeoff for the proposed scheme.

*Remark 1:* It should be noted that, while this paper focuses on a single-link scenario, the proposed technique can be readily extended to a multiuser DL scenario, where the DLT and the related RSM take place on a per-user basis, as facilitated by the ZF-TPC employed at the BS.

*Remark 2:* The proposed scheme does not consist of a power allocation scheme in the sense of allocating power according to the quality-of-service (QoS) requirements of the user. This power allocation may be applied in addition to the proposed scheme in the multiuser scenario, where different users with different QoS requirements employ different sets of power levels $\{P_1, P_2\}$ accordingly.

*Remark 3:* To facilitate the proposed power-level modulation, this paper focuses on phase shift keying (PSK) in terms of the classical symbol modulation. Its adaptation to quadrature amplitude modulation (QAM) is not trivial since the variability of the power levels for the classically modulated symbols would hinder the detection of the power levels of the spatially modulated symbols. Nevertheless, even for PSK modulation, our results illustrate a wide range of achievable BEs for the proposed scheme and an improved performance compared with classical SMX associated with both PSK and QAM for the same BE.

The remainder of this paper is organized as follows. Section II presents the MIMO system model and introduces the RSM transmission philosophy. Section III details the proposed DLT scheme, whereas in Section IV, we present our analytical study of the performance attained and the analytical optimization of the power ratio for the proposed scheme. Section V detail the complexity calculation and the study of the attainable PE. Finally, Section VI presents our numerical results, whereas our conclusions are offered in Section VII.

## II. SYSTEM MODEL AND RECEIVE-ANTENNA-BASED SPATIAL MODULATION

### A. System Model

Consider a MIMO system, where the transmitter and receiver are equipped with $N_t$ and $N_r$ antennas, respectively. For simplicity, unless stated otherwise, in this paper, we assume that the transmit power budget is limited as $P = 1$. For the case of the closed-form TPCs of [7]–[12], it is required that $N_t \geq N_r$. The given channel is modeled as follows:

$$\mathbf{y} = \mathbf{H}\mathbf{t} + \mathbf{w} \qquad (1)$$

where $\mathbf{y}$ is the vector of received symbols in all RAs, and $\mathbf{H}$ is the MIMO channel vector with elements $h_{m,n}$ representing the complex channel coefficient between the $n$th TA and the $m$th RA. Furthermore, $\mathbf{t}$ is the vector of precoded transmit symbols that will be discussed in the following, and $\mathbf{w} \sim \mathcal{CN}(0, \sigma^2 \mathbf{I})$ is the additive white Gaussian noise (AWGN) component at the receiver, with $\mathcal{CN}(\mu, \sigma^2)$ denoting the circularly symmetric complex Gaussian distribution with a mean of $\mu$ and a variance of $\sigma^2$.

### B. Receive-Antenna-Based Spatial Modulation

The block diagram of RSM as proposed in [36] is shown in Fig. 1(a). RSM targets a subset of the RAs by sending information symbols to these RAs and zero power to the rest of the RAs. While for RSM all RAs have to be on to detect the arrival of information symbols, for coherence with the SM literature, we shall refer to the antennas as "active" and "inactive," depending on whether they do or do not receive information symbols, respectively. The specific combination of RAs that do receive symbols implicitly conveys the symbol transmitted in the spatial domain. The above RA subset transmission is achieved by forming a supersymbol vector in the form $\mathbf{s}_m^k = \mathbf{e}_k b_m = [0, \ldots, b_{m_1}, \ldots, 0, \ldots, b_{m_2}, \ldots, 0]^T$ with $N_a$ nonzero elements, where $\mathbf{e}_k$ is a diagonal matrix of size
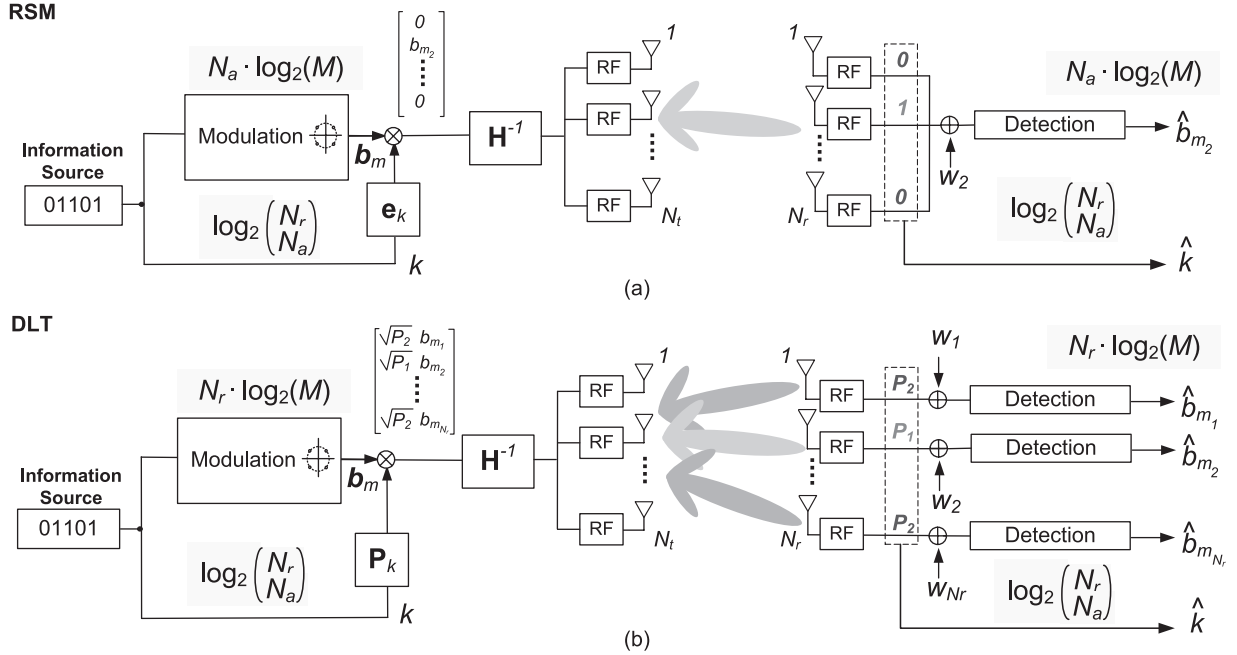
Fig. 1. Block diagram of (a) RSM and (b) DLT transmission.

$N_r$ with elements taken from the set $\{1, 0\}$ on its diagonal, which represents the RAs that are activated. The notation $[\cdot]^T$ denotes the transpose operator. Here, $b_{m_i}, m_i \in \{1, \ldots, M\}$ is a symbol taken from an $M$-order modulation alphabet that represents the transmitted waveform in the baseband domain conveying $\log_2(M)$ bits and $k$ represents the index of the $N_a$ activated RAs (the index of the nonzero elements in $\mathbf{s}_m^k$) conveying $\log_2 \binom{N_r}{N_a}$ bits in the spatial domain. Accordingly, the total number of bits conveyed per supersymbol for RSM is

$$\beta = N_a \log_2(M) + \log_2 \binom{N_r}{N_a}. \qquad (2)$$

The transmitter then sends

$$\mathbf{t} = f\mathbf{T}\mathbf{s}_m^k \qquad (3)$$

where $\mathbf{T} = \mathbf{H}^H(\mathbf{H}\mathbf{H}^H)^{-1}$ is the ZF-TPC [7] that preserves the form of $\mathbf{s}_m^k$ at the receiver. The factor $f = \sqrt{1/\text{tr}(\mathbf{T}\mathbf{T}^H)}$, where $\text{tr}(\cdot)$ denotes the trace operator and normalizes the average transmit power to $P = 1$. The received symbol vector can be written as

$$\mathbf{y} = f\mathbf{H}\mathbf{T}\mathbf{s}_m^k + \mathbf{w} = f\mathbf{s}_m^k + \mathbf{w} \qquad (4)$$

where, clearly, all IAI is removed. At the receiver, a joint ML detection of both the RA index and the transmit symbol is obtained by the following minimization:

$$[\hat{s}_m, \hat{k}] = \arg\min_i \|\mathbf{y} - \dot{\mathbf{y}}_i\|$$
$$= \arg\min_{m_i, k_i} \|\mathbf{y} - f\mathbf{H}\mathbf{T}\mathbf{s}_{m_i}^{k_i}\| \qquad (5)$$

where $\|\mathbf{x}\|$ denotes the norm of vector $\mathbf{x}$, and $\dot{\mathbf{y}}_i$ is the $i$th constellation point in the received SM constellation. A low-

complexity decoupled approach is also proposed in [36], where the first active antenna indexes are detected in the form of

$$\hat{k} = \arg\max_{j \in \mathcal{J}} \sum_{i=1}^{N_a} |y_{j,i}|^2 \qquad (6)$$

where $\mathcal{J}$ denotes the set of symbols in the spatial domain, and then, the classic modulated symbols are detected by

$$\hat{b}_{m_i} = \arg\min_{n_i \in \mathcal{Q}} |y_{\hat{k},i}/f - b_{n_i}|^2 \qquad (7)$$

where $\mathcal{Q}$ denotes the modulation constellation, and $b_{n_i}$ are the symbols in the modulated symbol alphabet. For reasons of computational complexity, we shall focus on the latter detector in this paper.

### III. PROPOSED DUAL-LAYERED TRANSMISSION

From the above system description, it can be seen that for the particular case of RSM, while the detection complexity is clearly reduced with respect to SMX, there are no savings in RF complexity since all $N_r$ RAs have to be activated and receiving for the detection in (6) and (7). Still, by forming a subset of beams towards the receiver, as shown in Fig. 1(a), the BE, i.e., the number of bits per channel use, is generally lower for RSM than for SMX. Motivated by this, we propose a dual-layered approach combining SMX with RSM, where the BE of conventional SMX MIMO transmission is strictly enhanced by encoding spatial bits in the RSM fashion in the received power domain, by selecting two distinct, nonzero power levels for the transmitted supersymbols instead of the "on–off" RSM transmission in the $\{1, 0\}$ manner. This allows for nonzero elements throughout the supersymbol vector $\mathbf{s}_m^k$,

hence supporting a full SMX transmission in the modulated signal domain. The block diagram of the proposed DLT is shown in Fig. 1(b).

*1) Transmitter:* Here, we employ a full data vector in the form of $\mathbf{b}_m = [b_{m_1}, b_{m_2}, \ldots, b_{m_{N_r}}]^T$, with all elements being nonzero, and the encoding of the spatial bits is achieved by allocating different power levels to the received symbols according to the spatial symbol $k$, by applying the power allocation matrix $\mathbf{P}_k$, i.e.,

$$\mathbf{s}_m^k = \mathbf{P}_k \mathbf{b}_m = [s_{m_1}, s_{m_2}, \ldots, s_{m_{N_r}}]^T \quad (8)$$

with

$$\mathbf{P}_k = \begin{bmatrix} \sqrt{p_1} & 0 & \cdots & 0 \\ 0 & \sqrt{p_2} & \cdots & 0 \\ \vdots & \vdots & \ddots & \vdots \\ 0 & 0 & \cdots & \sqrt{p_{N_r}} \end{bmatrix} \quad (9)$$

where $p_i, i \in [1, N_r]$ are taken from the set $\{P_1, P_2\}$ according to the spatial symbol $k$. Note that classic QoS-based power allocation can be applied in addition to this process by employing an additional power allocation matrix on top of (9). The receiver can then remove this additional matrix by simple inversion, in order to detect the spatial symbol. For notational simplicity and to keep the focus of the discussion on the proposed concept, we neglect QoS-based power allocation.

*2) Receiver:* At the receiver side, the explicit knowledge of the power levels $\{P_1, P_2\}$ is not required, as long as the detector can distinguish between the two power levels. The received signal of (4) can be decomposed as

$$y_p = f\sqrt{P_1} b_{m_p} + w_p, p \in \mathcal{A} \quad (10)$$

$$y_q = f\sqrt{P_2} b_{m_q} + w_q, q \in \mathcal{I} \quad (11)$$

where $\mathcal{A}$ and $\mathcal{I}$ denote the sets of "active" and "inactive" antennas, respectively. Hence, the receive processing is similar to the conceived one for RSM, with the difference that the classic modulated symbols of all RAs have to be detected, as opposed to those of $N_a$ antennas only for RSM. Accordingly, the receiver first detects the set of antennas with the highest received power levels and then detects the classic modulated symbols at all RAs according to

$$\hat{k} = \arg\max_{j \in \mathcal{J}} \sum_{i=1}^{N_a} |y_{j,i}|^2 \quad (12)$$

where $\mathcal{J}$ denotes the set of symbols in the spatial domain, and

$$\hat{\mathbf{b}}_m = \arg\min_{n \in \mathcal{Q}} |\mathbf{y}/f - \mathbf{b}_n|^2 \quad (13)$$

where $\mathcal{Q}$ denotes the classic modulation constellation, and $b_n$ are the symbols in the modulated symbol alphabet.

TABLE I
BE IN BITS PER CHANNEL USE FOR SMX, RSM, AND DLT

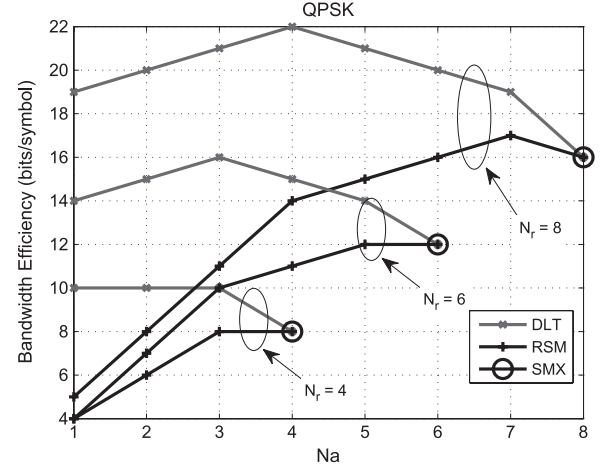| | Bandwidth Efficiency (BE) |
|---|---|
| SMX | $\beta = N_r \log_2(M)$ |
| RSM | $\beta = N_a \log_2(M) + \log_2\binom{N_r}{N_a}$ |
| DLT | $\beta = N_r \log_2(M) + \log_2\binom{N_r}{N_a}$ |



Fig. 2. BE versus $N_a$ for SMX, RSM, and DLT using the expressions of Table I.

### A. Bandwidth Efficiency

Clearly, the encoding process in (8) and (9) encodes $N_r \log_2(M)$ bits in the modulated symbol domain and an additional $\log_2\binom{N_r}{N_a}$ bits in the spatial domain. This results in a total of

$$\beta = N_r \log_2(M) + \log_2\binom{N_r}{N_a} \quad (14)$$

bits per transmitted supersymbol for DLT, which is strictly greater than that for SMX and RSM. Here, the notation $N_a$ denotes the number of antennas receiving symbols at the power level $P_1$. We should emphasize that, although all RAs are active for both RSM and the proposed DLT, for coherence with the SM literature, we shall adhere to the terms "active" and "inactive" to indicate the antennas receiving $\{1, 0\}$ and $\{P_1, P_2\}$ for RSM and DLT, respectively. A comparison of the BEs of SMX, RSM, and DLT is shown in Table I, where it can be seen that the proposed DLT approach has an improved BE compared with the conventional approaches. This is quantified in Fig. 2, where the BE is expressed in terms of bits per channel use is shown with increasing numbers of "active" antennas $N_a$ for MIMO links with $N_r = 4$, $N_r = 6$, and $N_r = 8$, where the clear benefits of the proposed approach can be seen. It can be observed that the additional BE of DLT compared with SMX can be maximized by appropriately selecting the number of activated antennas according to

$$\tilde{N}_a = \arg\max_{N_a} \log_2\binom{N_r}{N_a} = N_r/2 \quad (15)$$

which is demonstrated in the figure.

## B. Symbol Power Levels

With regard to the resulting BER performance, the set of spatial power levels $\{P_1, P_2\}$ must be carefully selected so that they satisfy a combination of two constraints.

1) There is sufficient separation between the two power levels $P_1, P_2$ for correct detection of the "active" antennas and hence the spatial symbol $k$ in the presence of noise.
2) The symbols received with $P_2 < P_1$ that dominate the BER of the modulated symbol detection must experience a sufficiently high signal-to-noise ratio (SNR) that is adequate for reliable demodulation.

Let us therefore define the power ratio

$$\alpha = \frac{P_2}{P_1} \qquad (16)$$

as the ratio between the two power levels transmitted, which is optimized in the following results. Since $N_a$ symbols are transmitted with power $P_1$ and the remaining $N_r - N_a$ symbols have power of $P_2$, given a total power budget of $P = 1$, we have

$$P_1 = \frac{1}{(N_r - N_a)\alpha + N_a} \qquad (17)$$

$$P_2 = \frac{\alpha}{(N_r - N_a)\alpha + N_a}. \qquad (18)$$

Clearly, since the power levels $P_1, P_2$ influence the reliability of detection for the modulated symbols and since the ratio $\alpha$ determines the detection reliability of the spatial symbols, $\alpha$ can be optimized for best BER performance. In the following, we derive a closed-form expression for the optimum $\alpha$ value for an $M$-order PSK modulation, where it can be seen that this optimum value is independent of both $N_r$ and of $N_a$.

*Remark:* Regarding the effect of the above on the transmit power distribution, we note that the power imbalance discussed refers to the information symbols $\mathbf{s}_m^k$ and does not translate to a power imbalance for the transmit symbols $\mathbf{t}$. Indeed, the ZF-precoded transmit symbols have the same average transmit power, constrained by the scaling factor $f$ as shown above, which is valid for both the proposed DLT and for the conventional SMX, and these transmit symbols exhibit the same power distribution for both techniques. In other words, the proposed scheme does not impact the design of the power amplifiers used at the transmitter.

To verify the above, Fig. 3 shows the probability density function (pdf) of the normalized transmit power per antenna for both SMX and DLT in a $(8 \times 4)$ element MIMO system. It can be seen that, as expected, both techniques show the same distribution of transmit power.

## IV. DUAL-LAYERED TRANSMISSION PERFORMANCE ANALYSIS AND OPTIMUM POWER RATIO $\alpha$

### A. Probability of Error

Here, we carry out a performance analysis for the proposed DLT scheme by deriving the PEP between the pair of symbols



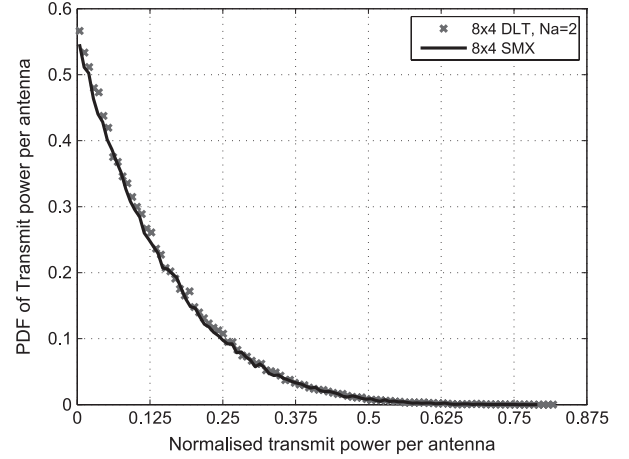Fig. 3. PDF of transmit power per antenna for a $(8 \times 4)$ MIMO with SMX and DLT and QPSK with Rayleigh fading.

$\mathbf{s}_m^k$ and $\mathbf{s}_n^l$ in the superimposed spatial and classic modulation constellations, following the analysis in [36]. Accordingly, we define the PEP as $\mathcal{P}(\mathbf{s}_m^k \to \mathbf{s}_n^l)$ and use the union bound for the average bit error probability $P_e$, which is expressed as

$$P_e \leq \frac{1}{\beta} E \left\{ \sum_{\mathbf{s}_m^k \in \mathcal{B}} \sum_{\mathbf{s}_n^l \in \mathcal{B} \neq \mathbf{s}_m^k} d\left(\mathbf{s}_m^k, \mathbf{s}_n^l\right) \mathcal{P}\left(\mathbf{s}_m^k \to \mathbf{s}_n^l\right) \right\} \qquad (19)$$

where $d(\mathbf{s}_m^k, \mathbf{s}_n^l)$ is the Hamming distance between the bit representations of symbols $\mathbf{s}_m^k, \mathbf{s}_n^l$ and $\mathcal{B} = \mathcal{J} \cup \mathcal{Q}$ is the supersymbol constellation defined as the union of the spatial domain constellation and the classic modulation constellation. We have used the operator $\cup$ to define the union of sets. For the PEP, we have the following theorem.

*Theorem 1:* The PEP $\mathcal{P}(\mathbf{s}_m^k \to \mathbf{s}_n^l)$ for DLT can be expressed as

$$\mathcal{P}(\mathbf{s}_m^k \to \mathbf{s}_n^l) = Q\left(\frac{f}{\sqrt{N_0}}\left(1 - \sum_{i=1}^{N_r} \sqrt{p_{k_i} p_{l_i}} \mathcal{R}\{b_{m_i}^* b_{n_i}\}\right)\right) \qquad (20)$$

where $Q(\cdot)$ denotes the Gaussian $q$-function [42], $\mathcal{R}\{\cdot\}$ denotes the real part of a number, $(\cdot)^*$ denotes the complex conjugate operation, and $N_0 = 2\sigma^2$ is the noise power spectral density.

*Proof:* Let us first define $\mathbf{r} = \mathbf{y}/f$ and $\mathbf{v} = \mathbf{w}/f$ for use in the following expressions. The PEP of the supersymbol constellation can be expressed as

$$\mathcal{P}\left(\mathbf{s}_m^k \to \mathbf{s}_n^l\right) = \mathcal{P}\left(\left\|\mathbf{r} - \mathbf{s}_m^k\right\|^2 > \left\|\mathbf{r} - \mathbf{s}_n^l\right\|^2\right)$$

$$= \mathcal{P}\left(\sum_{i=1}^{N_r} p_{k_i}|b_{m_i}|^2 - 2\mathcal{R}\left\{r_i^* \sqrt{p_{k_i}} b_{m_i}\right\}\right.$$

$$\left. > \sum_{i=1}^{N_r} p_{l_i}|b_{n_i}|^2 - 2\mathcal{R}\left\{r_i^* \sqrt{p_{l_i}} b_{n_i}\right\}\right). \qquad (21)$$

Since, for PSK signals, we have $|b_{m_i}| = 1$, by rearranging the terms in the probability expression, (21) can be further

358 simplified as

$$\mathcal{P}\left(\mathbf{s}_m^k \to \mathbf{s}_n^l\right) = \mathcal{P}\left(\sum_{i=1}^{N_r} \mathcal{R}\left\{r_i^* \sqrt{p_{l_i}} b_{n_i}\right\} - \mathcal{R}\left\{r_i^* \sqrt{p_{k_i}} b_{m_i}\right\}\right.$$
$$\left. > \frac{\sum_{i=1}^{N_r} p_{l_i} - \sum_{i=1}^{N_r} p_{k_i}}{2}\right). \quad (22)$$

359 Since $\sum_{i=1}^{N_r} p_{l_i} = \sum_{i=1}^{N_r} p_{k_i} = 1$ and $r_i = \sqrt{p_{k_i}} b_{m_i} + v_i$, we
360 have

$$\mathcal{P}(\mathbf{s}_m^k \to \mathbf{s}_n^l) = \mathcal{P}\left(\sum_{i=1}^{N_r} \mathcal{R}\left\{\sqrt{p_{k_i}} b_{m_i}^* \sqrt{p_{l_i}} b_{n_i}\right\} + \mathcal{R}\left\{v_i^* \sqrt{p_{l_i}} b_{n_i}\right\}\right.$$
$$\left. > \sum_{i=1}^{N_r} p_{k_i} |b_{m_i}|^2 + \mathcal{R}\left\{v_i^* \sqrt{p_{k_i}} b_{m_i}\right\}\right)$$
$$= \mathcal{P}\left(\sum_{i=1}^{N_r} \mathcal{R}\left\{v_i^* (\sqrt{p_{l_i}} b_{n_i} - \sqrt{p_{k_i}} b_{m_i})\right\}\right.$$
$$\left. > 1 - \sum_{i=1}^{N_r} \sqrt{p_{k_i} p_{l_i}} \mathcal{R}\left\{b_{m_i}^* b_{n_i}\right\}\right). \quad (23)$$

361 Let us define the random variable $\chi \hat{=} \sum_{i=1}^{N_r} \mathcal{R}\{v_i^*(\sqrt{p_{l_i}} b_{n_i} -$
362 $\sqrt{p_{k_i}} b_{m_i})\}$ for which we have $\chi \in \mathcal{N}(0, AN_0/f^2)$ with

$$A = \frac{\sum_{i=1}^{N_r} p_{l_i} |b_{n_i}|^2 + p_{k_i} |b_{n_i}|^2}{2} = \frac{1}{2}\sum_{i=1}^{N_r} p_{l_i} + p_{k_i}. \quad (24)$$

363 For the unity transmit power assumed in this paper, it can be
364 seen from (24) that $A = 1$. Accordingly, for the PEP, we have

$$\mathcal{P}(\mathbf{s}_m^k \to \mathbf{s}_n^l) = \mathcal{P}\left(\chi > 1 - \sum_{i=1}^{N_r} \sqrt{p_{k_i} p_{l_i}} \mathcal{R}\left\{b_{m_i}^* b_{n_i}\right\}\right) \quad (25)$$

365 which, for $\chi \in \mathcal{N}(0, N_0/f^2)$, leads to (20). ∎

## B. Optimum Power Ratio $\alpha$

367 As mentioned earlier, the power ratio $\alpha$ determines the
368 reliability of detection for the spatial symbol, whereas the lower
369 power level $P_2$ dominates the BER performance of the classic
370 modulated symbols' detection. As the probability of error in
371 (19) is dominated by the maximum PEP, the optimum power
372 ratio should be selected as

$$\alpha_{\text{opt}} = \arg\min_{\alpha} \max_{\mathbf{s}_m^k, \mathbf{s}_n^l} \left\{\mathcal{P}\left(\mathbf{s}_m^k \to \mathbf{s}_n^l\right)\right\}. \quad (26)$$

373 To simplify the analysis, we shall treat the errors in the spatial
374 and classic modulated symbols separately. Accordingly, for the
375 maximum PEP $\mathcal{P}_m(s_{m_i}^k \to s_{m_i}^l)$ in the spatial domain only, we
376 have the following theorem.

377 *Theorem 2:* The maximum PEP $\mathcal{P}_m(s_{m_i}^k \to s_{m_i}^l)$ for the
378 spatial symbols in DLT can be expressed as

$$\mathcal{P}_m\left(s_{m_i}^k \to s_{m_i}^l\right) = Q\left(\frac{f}{\sqrt{N_0}} \cdot \frac{\sqrt{P_2} - \sqrt{P_1}}{2}\right). \quad (27)$$

379 *Proof:* The maximum PEP in the spatial domain involves
380 the adjacent symbols of different power levels in the supersym-
381 bol constellation and can be expressed as

$$\mathcal{P}_m\left(s_{m_i}^k \to s_{m_i}^l\right)$$
$$= \mathcal{P}\left(\left\|r_i - s_{m_i}^k\right\|^2 > \left\|r_i - s_{m_i}^l\right\|^2\right)$$
$$= \mathcal{P}\left(P_1 - 2\mathcal{R}\left\{r_i^* \sqrt{P_1} b_{m_i}\right\} > P_2 - 2\mathcal{R}\left\{r_i^* \sqrt{P_2} b_{m_i}\right\}\right)$$
$$(28)$$

382 where, using $r_i = \sqrt{p_{k_i}} b_{m_i} + v_i$, we get

$$\mathcal{P}_m\left(s_{m_i}^k \to s_{m_i}^l\right)$$
$$= \mathcal{P}\left(P_1 - 2P_1 |b_{m_i}|^2 - 2\mathcal{R}\left\{u_i^* \sqrt{P_1} b_{m_i}\right\}\right.$$
$$\left. > P_2 - 2\sqrt{P_1 P_2} |b_{m_i}|^2 - 2\mathcal{R}\left\{u_i^* \sqrt{P_2} b_{m_i}\right\}\right)$$
$$= \mathcal{P}\left(2(\sqrt{P_2} - \sqrt{P_1})\mathcal{R}\left\{u_i^* b_{m_i}\right\} > P_1 + P_2 - 2\sqrt{P_1 P_2}\right)$$
$$= \mathcal{P}\left(-\mathcal{R}\left\{u_i^* b_{m_i}\right\} > \frac{\sqrt{P_1} - \sqrt{P_2}}{2}\right). \quad (29)$$

383 Similarly to the given proof, we have used the fact
384 that $|b_{m_i}|^2 = 1$, and it can be seen that $\psi \hat{=} -\mathcal{R}\{u_i^* b_{m_i}\} \in$
385 $\mathcal{N}(0, N_0/f^2)$. Accordingly, for the minimum PEP in the spatial
386 constellation, we have

$$\mathcal{P}_m\left(s_{m_i}^k \to s_{m_i}^l\right) = \mathcal{P}\left(\psi > \frac{\sqrt{P_2} - \sqrt{P_1}}{2}\right) \quad (30)$$

387 which leads to (27). ∎

388 This indicates that the separation between $\{P_1, P_2\}$ should
389 be maximized for minimizing the errors in the spatial bits,
390 which are dominated by the distance between the pairs of adja-
391 cent symbols having different power levels $d_s = \sqrt{P_1} - \sqrt{P_2}$.
392 We therefore define the spatial function $f_S(\alpha)$ that accounts for
393 the dependence of the spatial errors on $\alpha$ as

$$f_S(\alpha) \triangleq \sqrt{P_1} - \sqrt{P_2} = \frac{1 - \sqrt{\alpha}}{\sqrt{(N_r - N_a)\alpha + N_a}}. \quad (31)$$

394 As regards to the classic modulated symbol errors, it is
395 known that the PSK error probability is given as [41]

$$\mathcal{P}\left(s_{m_i}^k \to s_{n_i}^k\right) = \mathcal{P}\left(\left\|r_i - s_{m_i}^k\right\|^2 > \left\|r_i - s_{n_i}^l\right\|^2\right)$$
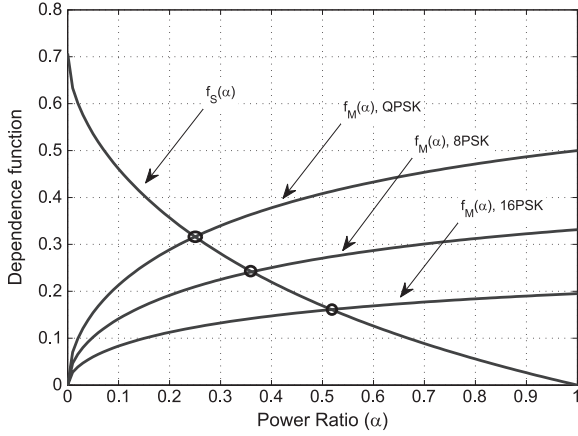$$= Q\left(f\sqrt{\frac{P_2}{N_0} \log_2(M)} \sin\frac{\pi}{M}\right). \quad (32)$$

Fig. 4. Theoretical optimization of $\alpha$ for DLT for a $(8 \times 4)$ MIMO with $N_a = 2$, using (36).

TABLE II
COMPLEXITY FOR SMX, RSM, AND THE PROPOSED DLT SCHEME.
$N_\chi = N_a$ FOR RSM, $N_\chi = N_r$ FOR DLT

| | Operations |
|---|---|
| *Transmitter:* | |
| ZF processing | $N_r^3 + 2N_t N_r$ |
| *Receiver:* | |
| Spatial detection | $2N_a \binom{N_r}{N_a}$ |
| Demodulation | $N_\chi M$ |
| **SMX Total** | $C_{SMX} = N_r^3 + N_r(2N_t + M)$ |
| **RSM Total** | $C_{RSM} = N_r^3 + 2N_t N_r + N_a \left( 2\binom{N_r}{N_a} + M \right)$ |
| **DLT Total** | $C_{DLT} = N_r^3 + N_r(2N_t + M) + 2N_a \binom{N_r}{N_a}$ |

Accordingly, we define the function $f_M(\alpha)$ for the dependence of the modulated symbol error on $\alpha$ as

$$f_M(\alpha) \triangleq \sqrt{P_2 \log_2(M) \sin \frac{\pi}{M}}$$
$$= \sqrt{\log_2(M) \sin \frac{\pi}{M} \cdot \frac{\alpha}{(N_r - N_a)\alpha + N_a}}. \quad (33)$$

The optimization (26) is equivalent to the maximization of the minimum of these functions:

$$\alpha_{\text{opt}} = \arg \max_\alpha \left\{ \min \left\{ f_S(\alpha), f_M(\alpha) \right\} \right\}. \quad (34)$$

The optimum power scaling ratio is, therefore, given as

$$\alpha_{\text{opt}} = \arg \max_\alpha \left\{ \frac{1 - \sqrt{\alpha}}{\sqrt{(N_r - N_a)\alpha + N_a}}, \right.$$
$$\left. \sqrt{\log_2(M) \sin \frac{\pi}{M} \cdot \frac{\alpha}{(N_r - N_a)\alpha + N_a}} \right\} \quad (35)$$

which is equivalent to selecting the factor $\alpha$ so that the two terms in the minimization become equal, which gives

$$\alpha_{\text{opt}} = \frac{1}{\left(1 + \sqrt{\log_2(M) \sin \frac{\pi}{M}}\right)^2}. \quad (36)$$

We examine this optimization in Fig. 4, which shows the functions $f_s(\alpha), f_M(\alpha)$ when increasing the values of $\alpha$ for the example of a $(8 \times 4)$-element DLT system with $N_a = 2$, for $M = 4, 8, 16$, i.e., quadrature phase-shift keying (QPSK), 8PSK, and 16PSK modulation. The intersections of the lines determine the optimum values of $\alpha$. It will be shown in the following that the theoretically obtained optimal values of $\alpha$ closely match the optimal values obtained by simulation.

## V. COMPLEXITY AND POWER EFFICIENCY

### A. Complexity

Here, we compare the computational complexity of SMX, RSM, and DLT and use this to carry out a comparison of the resulting PE of the techniques. First, Table II summarizes the computational complexity of each of the techniques, taking into account the dominant operations at the transmitter and receiver. We follow the typical assumption that multiplications and additions require an equal number of floating point operations. For all three schemes, the ZF-TPC employed at the transmitter involves the inversion of the channel matrix that requires $N_r^3 + N_t N_r$ operations and the multiplication with the supersymbol vector involving an additional $N_t N_r$ operations. At the receiver, all techniques require a demodulation stage that involves $M$ comparisons for and $M$-order modulation, for each antenna receiving information, i.e., $N_r M$ for both SMX and DLT, and $N_a M$ for RSM. The RSM and DLT require an additional stage for the detection of the spatial symbol which, from (6) involves $N_a$ complex multiplications and $N_a$ complex additions for each antenna combination out of the $\binom{N_r}{N_a}$ combinations in total.

### B. Power Efficiency

As the ultimate metric for evaluating the performance–complexity tradeoff and the overall usefulness of the proposed technique, we consider the PE of DLT compared with SMX and RSM. Following the modeling of [43]–[46], we define the PE of the communication link as the bit rate per total transmit power dissipated, i.e., the ratio of the goodput achieved over the power consumed:

$$\mathcal{E} = \frac{T}{P_{\text{PA}} + N_t \cdot P_t^{\text{RF}} + N_r \cdot P_r^{\text{RF}} + p_c \cdot C} \quad (37)$$

where $P_{\text{PA}} = ((\xi/\eta) - 1)P$ in Watts is the power dissipated by the power amplifier to produce the total transmit signal power $P$, with $\eta$ being the power amplifier's efficiency and $\xi$ being the modulation-dependent peak-to-average power ratio (PAPR). Furthermore, $P_t^{\text{RF}} = P_{\text{mix}} + P_{\text{filt}} + P_{\text{DAC}}$ and $P_r^{\text{RF}} = P_{\text{mix}} + P_{\text{filt}} + P_{\text{ADC}}$ represent the RF powers related to the mixers, to the transmit filters, to the digital-to-analog converter (DAC) at the transmitter and to the analog-to-digital converter (ADC) at the receiver, which are assumed to be constant for the purposes of this paper. We use practical values of these from [44] as $\eta = 0.35$ and $P_{\text{mix}} = 30.3$ mW, $P_{\text{filt}} = 2.5$ mW, $P_{\text{DAC}} = 1.6$ mW, and $P_{\text{DAC}} = 1.3$ mW, yielding $P_t^{\text{RF}} = 34.4$ mW, and $P_r^{\text{RF}} = 34.1$ mW. In (37), $p_c$ in Watts/KOps is the power per $10^3$ elementary

operations (KOps) of the digital signal processor, and $C$ is the number of operations involved, taken from Table II, where it is assumed that the operations shown dominate the digital signal processing complexity of the link. This term is used for introducing the complexity as a factor related to the power dissipation in the PE metric. Typical values of $p_c$ include $p_c = 22.88$ mW/KOps for the Virtex-4 and $p_c = 5.76$ mW/KOps for the Virtex-5 FPGA family from Xilinx [47]. Finally

$$T = \beta B(1 - P_B) = \beta B(1 - P_e)^B \qquad (38)$$

represents the achieved goodput, where $P_B$ is the block error rate with a block of size $B$ symbols, and $\beta$ is the BE of SM in bits per symbol, taken from Table I. For reference, we have assumed an LTE Type-2 TDD frame structure [48]. This has a 10 ms duration that consists of 10 subframes, out of which five subframes, containing 14 symbol time slots each, are used for DL transmission yielding a block size of $B = 70$ for the DL, whereas the remainder are used for both uplink (UL) and control information transmission. A slow fading channel is assumed where the channel remains constant for the duration of the frame.

The expression in (37) provides an amalgamated metric that combines goodput, complexity, and transmit signal power, all in a unified metric. High values of $\mathcal{E}$ indicate that high bit rates are achievable for a given power consumption and thus denote high energy efficiency. The following results show that DLT provides an increased energy efficiency compared with SMX and RSM in numerous scenarios using different transmit power levels $P$.

## VI. NUMERICAL RESULTS

To evaluate the benefits of the proposed technique, this section presents numerical results based on Monte Carlo simulations of SMX, RSM, and the proposed DLT. The channel impulse response is assumed perfectly known at the transmitter. Without loss of generality, unless stated otherwise, we assume that the transmit power is restricted to $P = 1$. MIMO systems with up to eight TAs employing QPSK and 8PSK modulation are explored, albeit it is plausible that the benefits of the proposed technique extend to larger scale systems and higher order modulation.

*Remark:* It should be noted that the BE improvement shown in the following could also be obtained by SMX with the aid of an increased classical modulation order. Accordingly, in the following, we compare the proposed DLT to: (a) SMX using the same classical modulation order to illustrate the improved BE of DLT; and (b) SMX relying on a higher modulation order to highlight the improved performance of DLT for an identical BE.

In Fig. 5, we show the BER as a function of the power ratio for DLT for the $(8 \times 4)$ MIMO system, where the values of $\alpha$ in the area of 0.25 can be seen to provide the best performance. This matches well with the theoretically derived result of Section IV-A and Fig. 4. Similarly, Fig. 6 shows the BER versus $\alpha$ performance for higher order modulation 8PSK and 16PSK. Again, a close match can be seen with the theoretically derived values for $\alpha_{\mathrm{opt}}$. In Fig. 7, we show the BER with increasing SNR for the proposed DLT, where the black
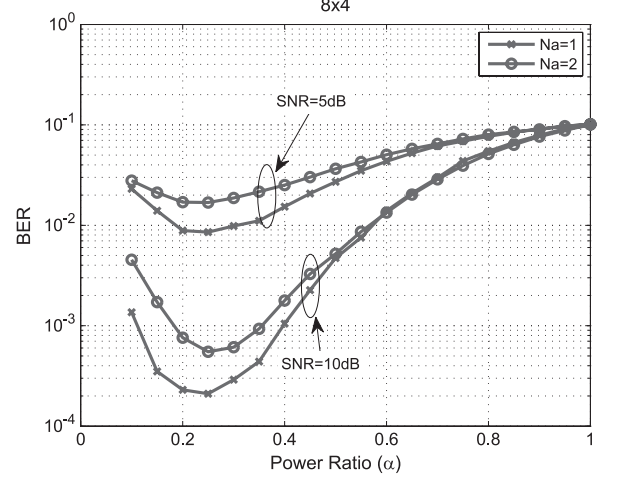


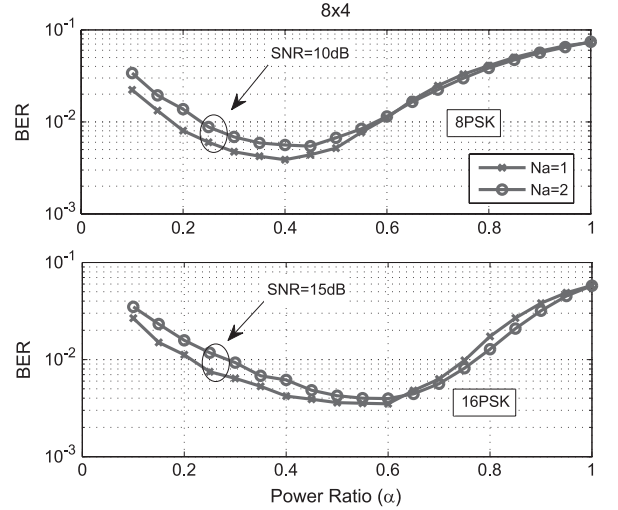Fig. 5. BER versus $\alpha$ for an $(8 \times 4)$ MIMO with SMX and DLT, as well as QPSK with Rayleigh fading.



Fig. 6. BER versus $\alpha$ for a $(8 \times 4)$ MIMO with DLT, as well as 8PSK and 16PSK with Rayleigh fading.
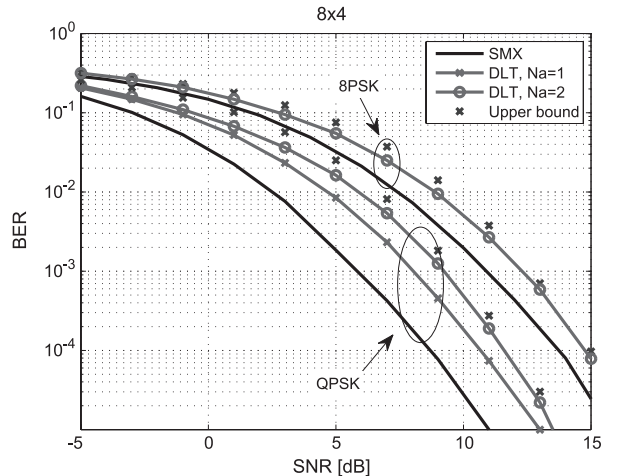


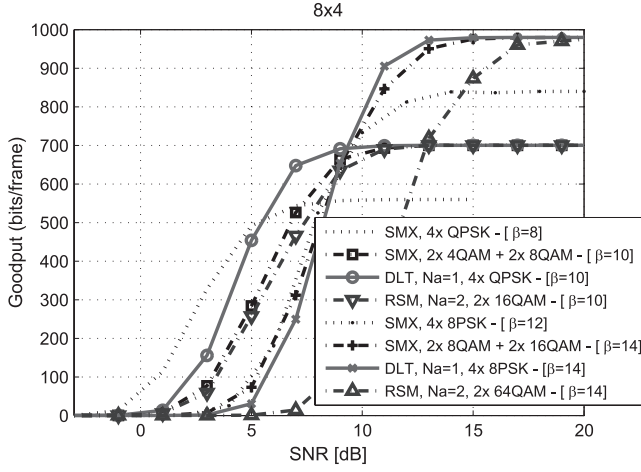Fig. 7. BER versus SNR for a $(8 \times 4)$ MIMO with SMX and DLT, as well as QPSK and 8PSK with Rayleigh fading.

Fig. 8. Goodput versus SNR for a $(8 \times 4)$ MIMO with SMX and DLT, as well as Rayleigh fading.
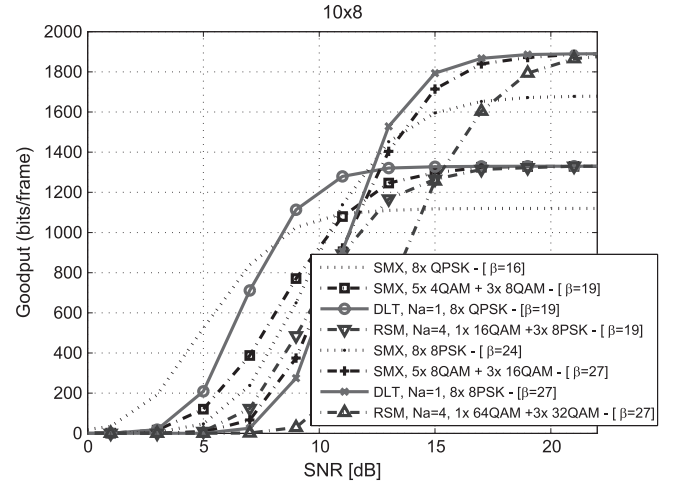


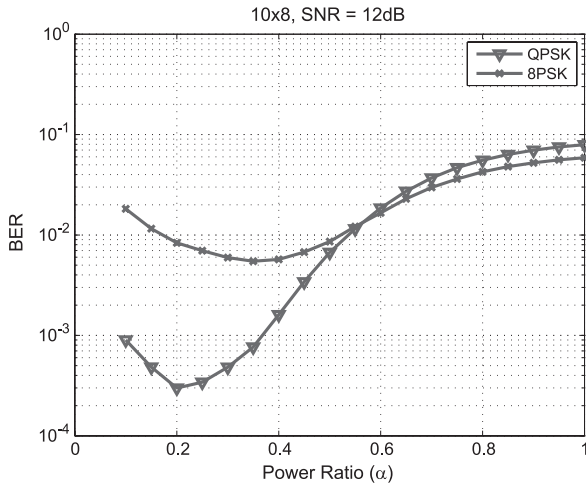Fig. 10. Goodput versus SNR for a $(10 \times 8)$ MIMO with SMX and DLT, as well as Rayleigh fading.



Fig. 9. BER versus $\alpha$ for a $(10 \times 8)$ MIMO with DLT, QPSK, and 8PSK with Rayleigh fading.
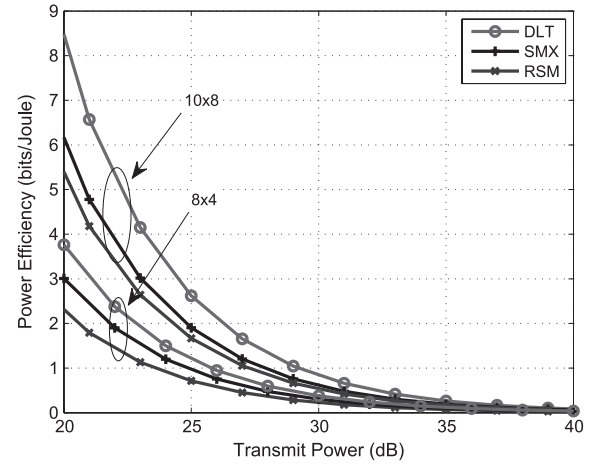


Fig. 11. PE versus transmit power for $(10 \times 8)$ and $(8 \times 4)$ MIMO systems with SMX and DLT, as well as QPSK with Rayleigh fading.

lines for $N_a = 4$ represent SMX transmission. The curves show results for both QPSK and 8PSK. The theoretical upper bound using (19) is also depicted for both cases, and it can be observed that it offers a tight bound. Clearly, the DLT scheme has inferior BER performance compared with SMX due to the additional spatial streams but at the benefit of improved BE. The improved BE of DLT is demonstrated in Fig. 8 where the goodput with increasing SNR is depicted for the same $(8 \times 4)$ MIMO scenario. Clearly, DLT provides higher goodput than SMX for sufficiently high SNR values. To complete our comparisons, for both scenarios in the figure, we also show the cases where the symbol modulation order used for SMX and RSM is increased for some of the spatial streams in order to achieve the same BE values of $\beta = 10$ and $\beta = 14$ with the proposed DLT, for QPSK and 8PSK, respectively. Clearly, this has an impact on the SNR requirement of SMX, where it can be seen that the proposed DLT scheme obtains the maximum goodput at lower SNR values.

The performance comparison is extended to the $(10 \times 8)$ MIMO system in Figs. 9 and 10. In Fig. 9, we show the

BER as a function of the power ratio for DLT, where the best performance is provided for $\alpha$ in the range of 0.2 for QPSK and 0.4 for 8PSK. Fig. 10 shows the goodput with increasing SNR, where again it can be observed that the DLT provides better goodput than SMX at higher SNR values. As above, for both scenarios characterized in the figure, we also include the cases where the symbol modulation order used for SMX and RSM is increased for some of the spatial streams in order to achieve the same BE values of $\beta = 19$ and $\beta = 27$ with the proposed DLT, for QPSK and 8PSK, respectively. Again, it can be seen that the proposed DLT scheme obtains the maximum goodput at lower SNR values.

Finally, Figs. 11 and 12 show the PE of the SMX, RSM and DLT techniques. Fig. 11 shows the PE for increasing transmit power, within the region of power values used in the communication standards for $(10 \times 8)$ and $(8 \times 4)$ MIMO systems. It is assumed here that the noise variance is $\sigma^2 = 1$ to indirectly account for the path loss (and, hence, the useful signal power loss) experienced in real transmission. It can be seen that the proposed DLT scheme outperforms SMX and RSM in terms
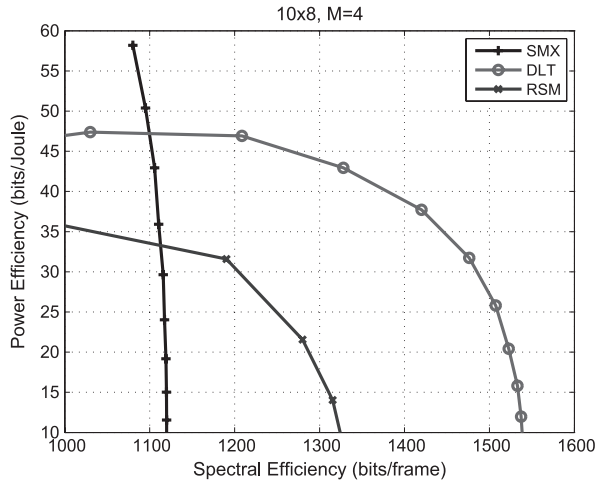
Fig. 12. Power efficiency versus spectral efficiency for a $(10 \times 8)$ MIMO with SMX and DLT, as well as QPSK with Rayleigh fading.

of PE for all transmit power values in both $(10 \times 8)$ and $(8 \times 4)$ MIMO systems. The tradeoff between PE and BE is shown in Fig. 12. It can be seen that DLT offers a more scalable tradeoff with a wider range of BEs for the PE range, while it is more power efficient than SMX and RSM in the region of high BEs.

## VII. CONCLUSION

A dual-layered DL transmission scheme was proposed, which combines traditional MIMO SMX with RSM. As opposed to traditional SM where a subset of antennas carry a spatial stream, here, we allow all antennas to carry information by applying SM on the symbol power-level domain. This provides scope for the analytical optimization of the ratio between the power levels used in the proposed scheme. Both our simulations and performance analysis show that, by allowing all antennas to form spatial streams, the proposed scheme improves the system's BE and power efficiency compared to both SMX and SM.

Further work can involve exploring more advanced TPC schemes for the proposed transmission scheme and exploring the adaptations of the proposed scheme for QAM and enhancing its robustness to channel state information errors.

## REFERENCES

[1]  D. Gesbert, M. Kountouris, R. Heath, C. Chae, and T. Salzer, "Shifting the MIMO paradigm," *IEEE Signal Process. Mag.*, vol. 24, no. 5, pp. 36–46, Sep. 2007.

[2]  M. Costa, "Writing on dirty paper," *IEEE Trans. Inf. Theory*, vol. IT-29, no. 3, pp. 439–441, May 1983.

[3]  C. Windpassinger, R. Fischer, T. Vencel, and J. Huber, "Precoding in multiantenna and multiuser communications," *IEEE Trans. Wireless Commun.*, vol. 3, no. 4, pp. 1305–1316, Jul. 2004.

[4]  C. Masouros, M. Sellathurai, and T. Rantarajah, "Interference optimization for transmit power reduction in Tomlinson–Harashima precoded MIMO downlinks," *IEEE Trans. Signal Process.*, vol. 60, no. 5, pp. 2470–2481, May 2012.

[5]  A. Garcia and C. Masouros, "Power loss reduction for MMSE-THP with multidimensional symbol scaling," *IEEE Commun. Lett.*, vol. 18, no. 7, pp. 1147–1150, Jul. 2014.

[6]  A. Garcia and C. Masouros, "Power-efficient Tomlinson–Harashima precoding for the downlink of multi-user MISO systems," *IEEE Trans. Commun.*, vol. 62, no. 6, pp. 1884–1896, Jun. 2014.

[7]  C. B. Peel, B. M. Hochwald, and A. L. Swindlehurst, "A vector-perturbation technique for near-capacity multiantenna multiuser communication—Part I: Channel inversion and regularization," *IEEE Trans. Commun.*, vol. 53, no. 1, pp. 195–202, Jan. 2005.

[8]  C. Masouros and E. Alsusa, "Dynamic linear precoding for the exploitation of known interference in MIMO broadcast systems," *IEEE Trans. Wireless Commun.*, vol 8, no. 3, pp. 1396–1404, Mar. 2009.

[9]  C. Masouros and E. Alsusa, "Soft transmitter precoding for the downlink of DS/CDMA communication systems," *IEEE Trans. Veh. Technol.*, vol. 59, no. 1, pp. 203–215, Jan. 2010.

[10]  C. Masouros, T. Ratnarajah, M. Sellathurai, C. Papadias, and A. Shukla, "Known interference in wireless communications: A limiting factor or a potential source of green signal power?" *IEEE Commun., Mag.*, vol. 51, no. 10, pp. 162–171, Oct. 2013.

[11]  G. Zheng *et al.*, "Rethinking the role of interference in wireless networks," *IEEE Commun. Mag.*, vol. 52, no. 11, pp. 152,158, Nov. 2014.

[12]  C. Masouros, "Correlation rotation linear precoding for MIMO broadcast communications," *IEEE Trans. Signal Process.*, vol 59, no. 1, pp. 252–262, Jan. 2011.

[13]  F. Rusek *et al.*, "Scaling up MIMO: Opportunities and challenges with very large arrays," *IEEE Signal Process. Mag.*, vol. 30, no. 1, pp. 40–60, Jan. 2013.

[14]  C. Masouros, M. Sellathurai, and T. Ratnarajah, "Large-scale MIMO transmitters in fixed physical spaces: The effect of transmit correlation and mutual coupling," *IEEE Trans. Commun.*, vol. 61, no. 7, pp. 2794–2804, Jul. 2013.

[15]  C. Masouros and M. Matthaiou, "Physically constrained massive MIMO: Hitting the wall of favorable propagation," *IEEE Commun. Let.*, vol. 19, no. 5, pp. 771–774, May 2015.

[16]  R. Mesleh, H. Haas, S. Sinanovic, C. W. Ahn, and S. Yun, "Spatial modulation," *IEEE Trans. Veh. Technol.*, vol. 57, no. 4, pp. 2228–2241, Jul. 2008.

[17]  M. Di Renzo, H. Haas, A. Ghrayeb, S. Sugiura, and L. Hanzo, "Spatial modulation for generalized MIMO: Challenges, opportunities, and implementation," *Proc. IEEE*, vol. 102, no. 1, pp. 56–103, Jan. 2014.

[18]  A. Garcia and C. Masouros, "Low-complexity compressive sensing detection for spatial modulation in large-scale multiple access channels," *IEEE Trans. Commun.*, to be published.                                   AQ1

[19]  M. Di Renzo and H. Haas, "Bit error probability of space modulation over Nakagami-m fading: Asymptotic analysis," *IEEE Commun. Lett.*, vol. 15, no. 10, pp. 1026–1028, Oct. 2011.

[20]  J. Jeganathan, A. Ghrayeb, and L. Szczecinski, "Spatial modulation: Optimal detection and performance analysis," *IEEE Commun. Lett.*, vol. 12, no. 8, pp. 545–547, Aug. 2008.

[21]  A. Younis, S. Sinanovic, M. Di Renzo, R. Mesleh, and H. Haas, "Generalised sphere decoding for spatial modulation," *IEEE Trans. Commun.*, vol. 61, no. 7, pp. 2805–2815, Jul. 2013.

[22]  J. Wang, S. Jia, and J. Song, "Generalised spatial modulation system with multiple active transmit antennas and low complexity detection scheme," *IEEE Trans. Wireless Commun.*, vol. 11, no. 4, pp. 1605–1615, Apr. 2012.

[23]  M. Di Renzo and H. Haas, "On transmit diversity for spatial modulation MIMO: Impact of spatial constellation diagram and shaping filters at the transmitter," *IEEE Trans. Veh. Technol.*, vol. 62, no. 6, pp. 2507–2531, Jul. 2013.

[24]  P. Yang *et al.*, "Star-QAM signaling constellations for spatial modulation," *IEEE Trans. Veh. Technol.*, vol. 63, no. 8, pp. 3741–3749, Oct. 2014.

[25]  S. Sugiura, C. Xu, S. X. Ng, and L. Hanzo, "Reduced-complexity coherent versus non-coherent QAM-aided space-time shift keying," *IEEE Trans. Commun.*, vol. 59, no. 11, pp. 3090–3101, Nov. 2011.

[26]  K. Ntontin, M. Di Renzo, A. Perez-Neira, and C. Verikoukis, "Adaptive generalized space shift keying," *EURASIP J. Wireless Commun. Netw.*, vol. 2013, no. 1, p. 43, Feb. 2013.

[27]  S. Sugiura and L. Hanzo, "On the joint optimization of dispersion matrices and constellations for near-capacity irregular precoded space-time shift keying," *IEEE Trans. Wireless Commun.*, 2013, vol. 12, no. 1, pp. 380–387, Jan. 2013.

[28]  M. Maleki, H. Bahrami, S. Beygi, M. Kafashan, and N. H. Tran, "Space modulation with CSI: Constellation design and performance evaluation," *IEEE Trans. Veh. Technol.*, vol. 62, no. 4, pp. 1623–1634, May 2013.

[29]  X. Guan, Y. Cai, and W. Yang, "On the mutual information and precoding for spatial modulation with finite alphabet," *IEEE Wireless Commun. Lett.*, vol. 2, no. 4, pp. 383–386, Aug. 2013.

[30] J. M. Luna-Rivera, D. U. Campos-Delgado, and M. G. Gonzalez-Perez, "Constellation design for spatial modulation," *Procedia Technol.*, vol. 7, pp. 71–78, 2013.

[31] C. Masouros, "Improving the diversity of spatial modulation in MISO channels by phase alignment," *IEEE Commun. Lett.*, vol. 18, no. 5, pp. 729–732, May 2014.

[32] A. Garcia, C. Masouros, and L. Hanzo, "Pre-scaling optimization for space shift keying based on semidefinite relaxation," *IEEE Trans. Commun.*, to be published.

[33] C. Masouros and L. Hanzo, "Constellation-randomization achieves transmit diversity for single-RF spatial modulation," *IEEE Trans. Veh. Technol.*, to be published.

[34] J. Jeganathan, A. Ghrayeb, L. Szczecinski, and A. Ceron, "Space shift keying modulation for MIMO channels," *IEEE Trans. Wireless Commun.*, vol. 8, no. 7, pp. 3692–3703, Jul. 2009.

[35] M. Di Renzo and H. Haas, "Bit error probability of space modulation over Nakagami-m fading: Asymptotic analysis," *IEEE Commun. Lett.*, vol. 15, no. 10, pp. 1026–1028, Oct. 2011.

[36] R. Zhang, L. Yang, and L. Hanzo, "Generalised pre-coding aided spatial modulation," *IEEE Trans. Wireless Commun.*, vol. 12, no. 11, pp. 5434–5443, Nov. 2013.

[37] D.-T. Phan-Huy and M. Helard, "Receive antenna shift keying for time reversal wireless communications," in *Proc. IEEE ICC*, Jun. 2012, pp. 4852–4856.

[38] R. Zhang, L. L. Yang, and L. Hanzo, "Error probability and capacity analysis of generalised pre-coding aided spatial modulation," *IEEE Trans. Wireless Commun.*, vol. 14, no. 1, pp. 364–375, Jan. 2015.

[39] A. Stavridis, S. Sinanovic, M. Di Renzo, and H. Haas, "Transmit precoding for receive spatial modulation using imperfect channel knowledge," in *Proc. IEEE Veh. Technol. Conf. Spring*, May 2012, pp. 1–5.

[40] R. M. Legnain, R. H. M. Hafez, I. D. Marsland, and A. M. Legnain, "A novel spatial modulation using MIMO spatial multiplexing," in *Proc. ICCSPA*, Feb. 2013, pp. 1–4.

[41] J. G. Proakis, *Digital Communications*, Electrical Engineering, 3rd ed. New York, NY, USA: McGraw-Hill, 1995.

[42] M. Abramowitz and I. A. Stegun, *Handbook of Mathematical Functions With Formulas, Graphs, and Mathematical Tables*. New York, NY, USA: Dover, 1972.

[43] X. Cong, G. Y. Li, Z. Shunqing, Y. Chen, and S. Xu, "Energy- and spectral-efficiency tradeoff in downlink OFDMA networks," *IEEE Trans. Wireless Commun.*, vol. 10, no. 11, pp. 3874–3886, Nov. 2011.

[44] S. Cui, A. J. Goldsmith, and A. Bahai, "Energy-constrained modulation optimization," *IEEE Trans. Wireless Commun.*, vol. 4, no. 5, pp. 2349–2360, Sep. 2005.

[45] C. Masouros, M. Sellathurai, and T. Ratnarajah, "Computationally efficient vector perturbation precoding using thresholded optimization," *IEEE Trans. Commun.*, vol. 61, no. 5, pp. 1880–1890, May 2013.

[46] C. Masouros, M. Sellathurai, and T. Ratnarajah, "Vector perturbation based on symbol scaling for limited feedback MIMO downlinks," *IEEE Trans. Signal Process.*, vol. 62, no. 3, pp. 562–571, Feb. 1, 2014.

[47] D. Curd, Power consumption in 65 nm FPGAs, Xilinx White Paper, Feb. 2007.

[48] *Evolved Universal Terrestrial Radio Access (E-UTRA); LTE Physical Layer; General Description*, Third-Generation Partnership Project, TS 36.201, V11.1.0 (2008-03), Rel. 11, 2008.

**Christos Masouros** (M'06–SM'14) received the Diploma in electrical and computer engineering from the University of Patras, Patras, Greece, in 2004 and the M.Sc. and Ph.D. degrees in electrical and electronic engineering from The University of Manchester, Manchester, U.K., in 2006 and 2009, respectively.

He was a Research Associate with the University of Manchester and a Research Fellow with Queen's University Belfast, Belfast, U.K. He is currently a Lecturer with the Department of Electrical and Electronic Engineering, University College London, London, U.K. His research interests include wireless communications and signal processing, with particular focus on green communications, large-scale antenna systems, cognitive radio, and interference mitigation techniques for multiple-input–multiple-output and multicarrier communications.

Dr. Masouros is the Principal Investigator of the EPSRC Project EP/M014150/1 on large-scale antenna systems. He received a Royal Academy of Engineering Research Fellowship for 2011–2016.

**Lajos Hanzo** (M'91–SM'92–F'04) received the M.S. degree in electronics and the Ph.D. degree from Budapest University of Technology and Economics (formerly, Technical University of Budapest), Budapest, Hungary, in 1976 and 1983, respectively; the D.Sc. degree from the University of Southampton, Southampton, U.K., in 2004; and the "Doctor Honoris Causa" degree from Budapest University of Technology and Economics in 2009.

During his 38-year career in telecommunications, he has held various research and academic posts in Hungary, Germany, and the U.K. Since 1986, he has been with the School of Electronics and Computer Science, University of Southampton, where he holds the Chair in Telecommunications. He is currently directing a 100-strong academic research team, working on a range of research projects in the field of wireless multimedia communications sponsored by industry, the Engineering and Physical Sciences Research Council of U.K., the European Research Council's Advanced Fellow Grant, and the Royal Society Wolfson Research Merit Award. During 2008–2012, he was a Chaired Professor with Tsinghua University, Beijing, China. He is an enthusiastic supporter of industrial and academic liaison and offers a range of industrial courses. He has successfully supervised more than 80 Ph.D. students, coauthored 20 John Wiley/IEEE Press books on mobile radio communications, totaling in excess of 10 000 pages, and published more than 1400 research entries on IEEEXplore. He has more than 20 000 citations. His research is funded by the European Research Council's Senior Research Fellow Grant.

Dr. Hanzo is a Fellow of the Royal Academy of Engineering, The Institution of Engineering and Technology, and the European Association for Signal Processing. He is also a Governor of the IEEE Vehicular Technology Society. He has served as the Technical Program Committee Chair and the General Chair of IEEE conferences, has presented keynote lectures, and has been awarded a number of distinctions. During 2008–2012, he was the Editor-in-Chief of the IEEE Press.

# AUTHOR QUERIES

AUTHOR PLEASE ANSWER ALL QUERIES

AQ1 = Please provide publication update in Ref. [18].
AQ2 = Please provide publication update in Ref. [32].
AQ3 = Please provide publication update in Ref. [33].

END OF ALL QUERIES